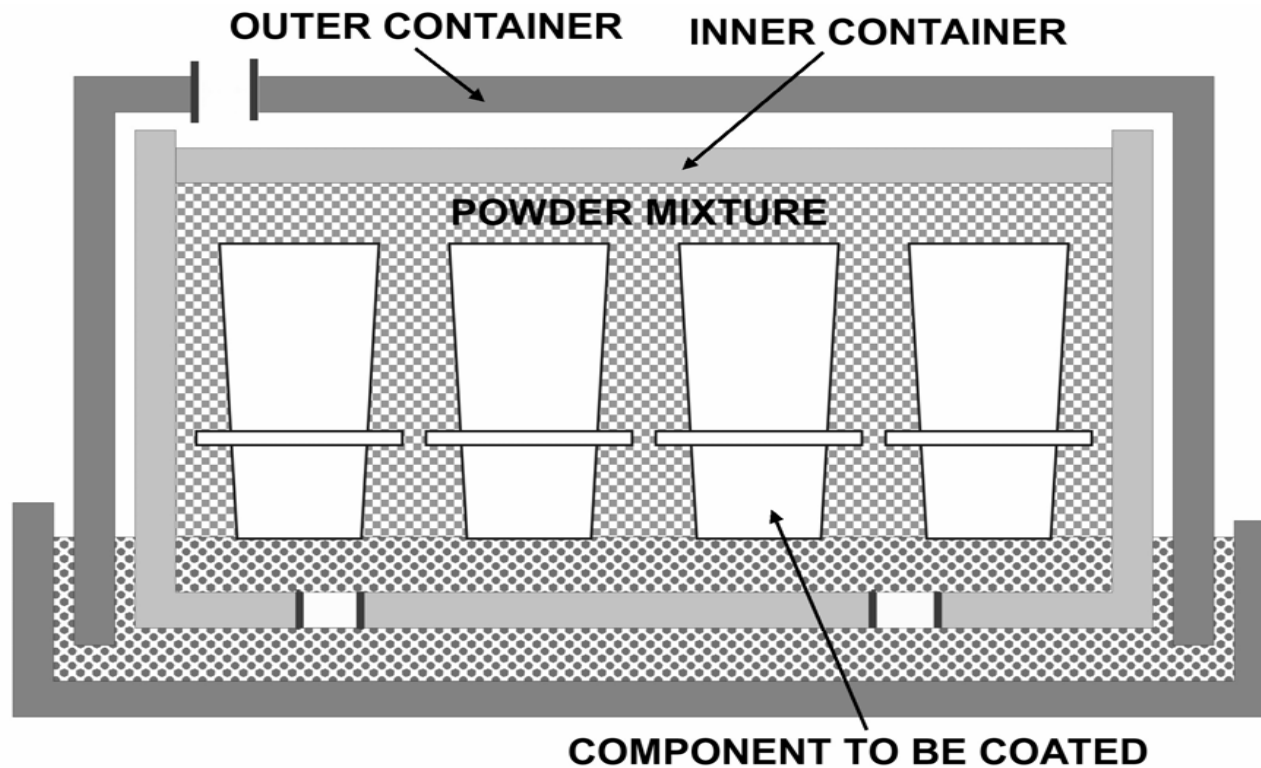


4. Advanced Coatings and Claddings

- a. Application Techniques
- b. Coating Durability
 - Limitations
 - Lifetime Prediction

Coating Deposition Techniques



**Schematic Diagram of the Pack
Cementation Process**

Pack Cementation

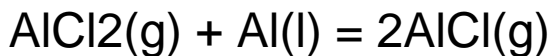
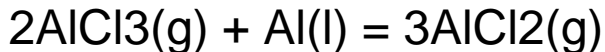
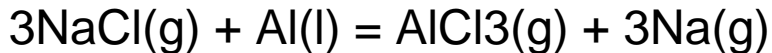
Pack Components

Source (Cr, Al, Si or their alloys)

Activator (NaCl, NH₄Cl or other halide)

Inert Filler (often alumina)

Reactions between Source and Activator (Aluminizing)



Deposition on Substrate (Aluminizing)

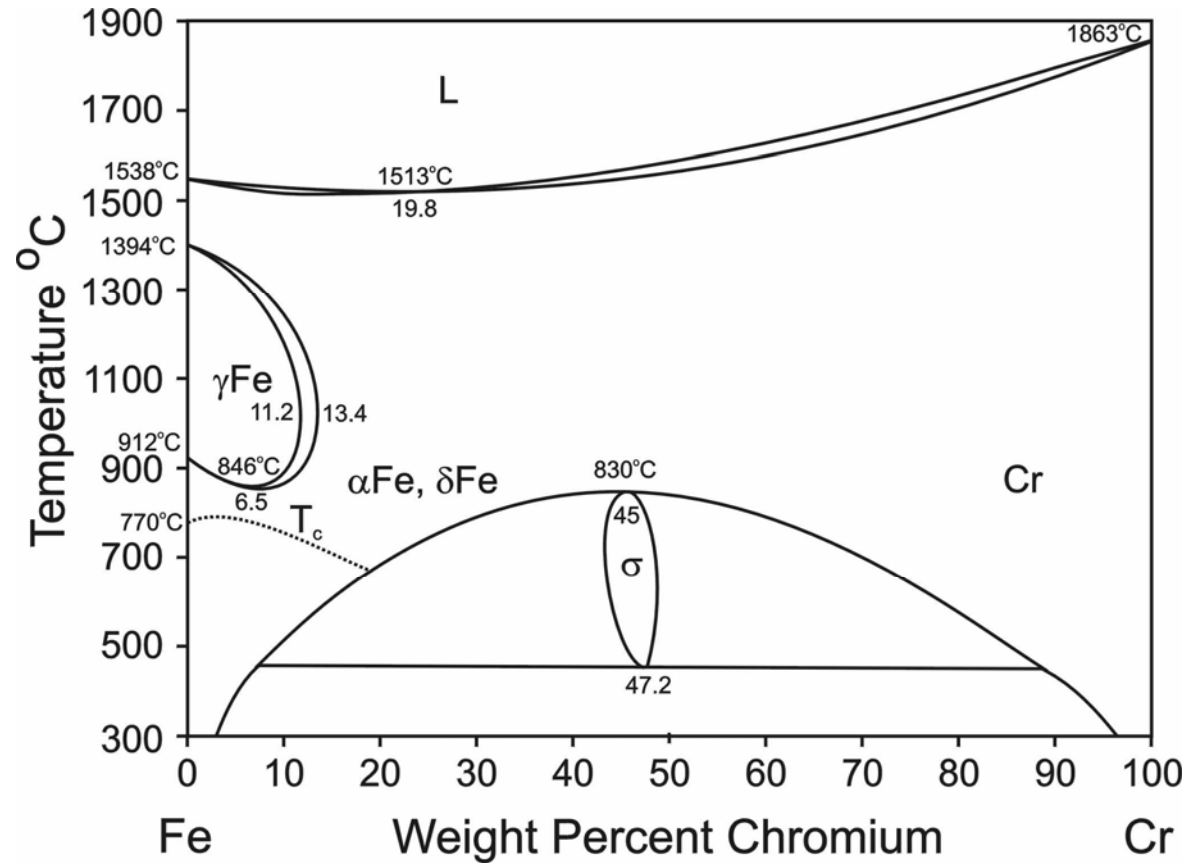


And, for activators which contain hydrogen e.g. NH₄Cl,

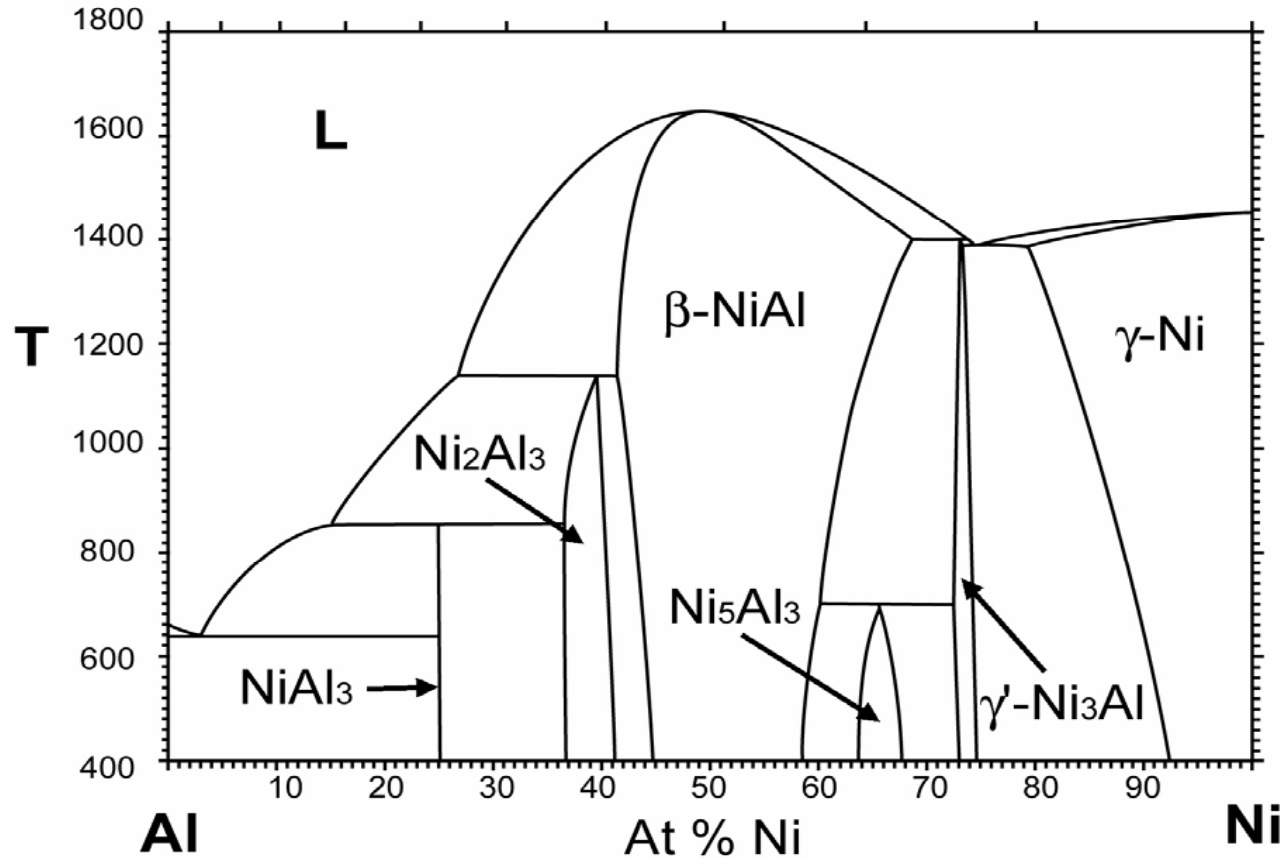


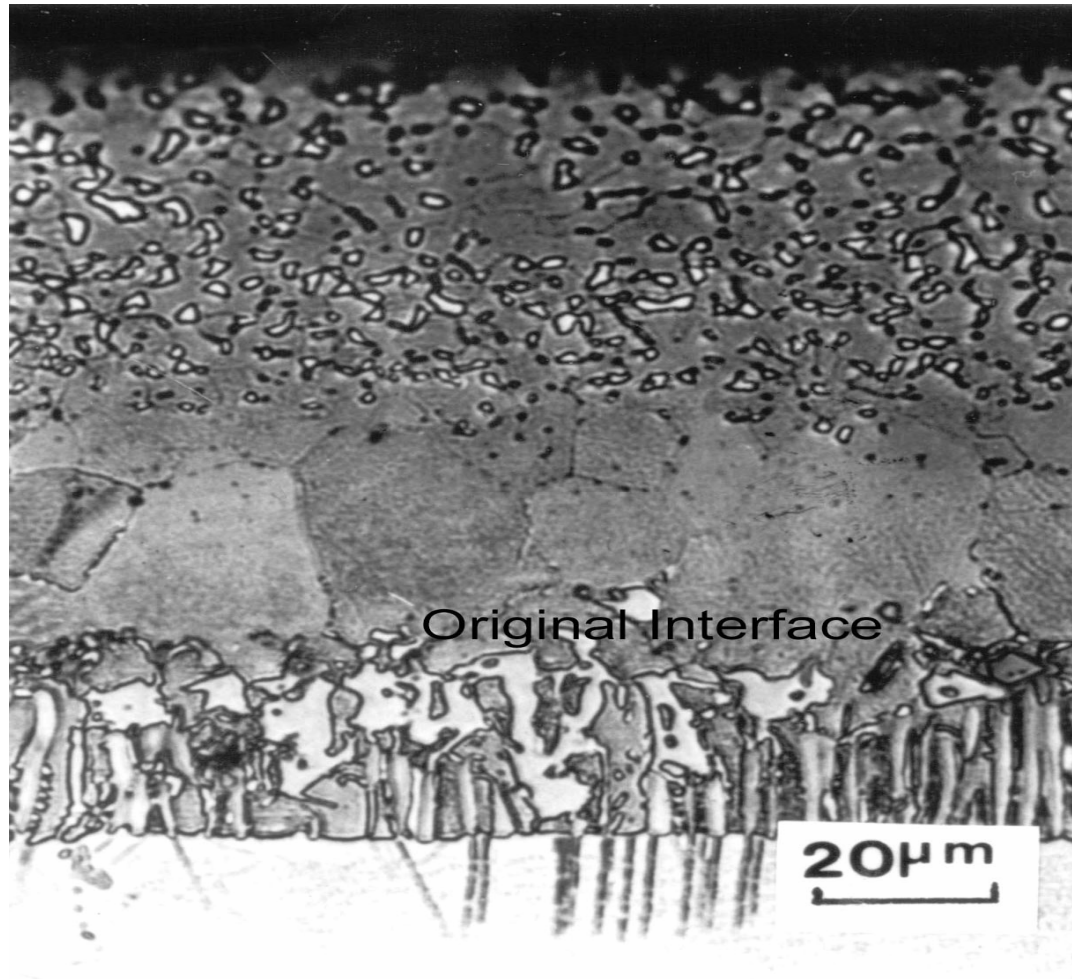
(The underlined symbols refer to species in the solid substrate.)

Fe-Cr Phase Diagram

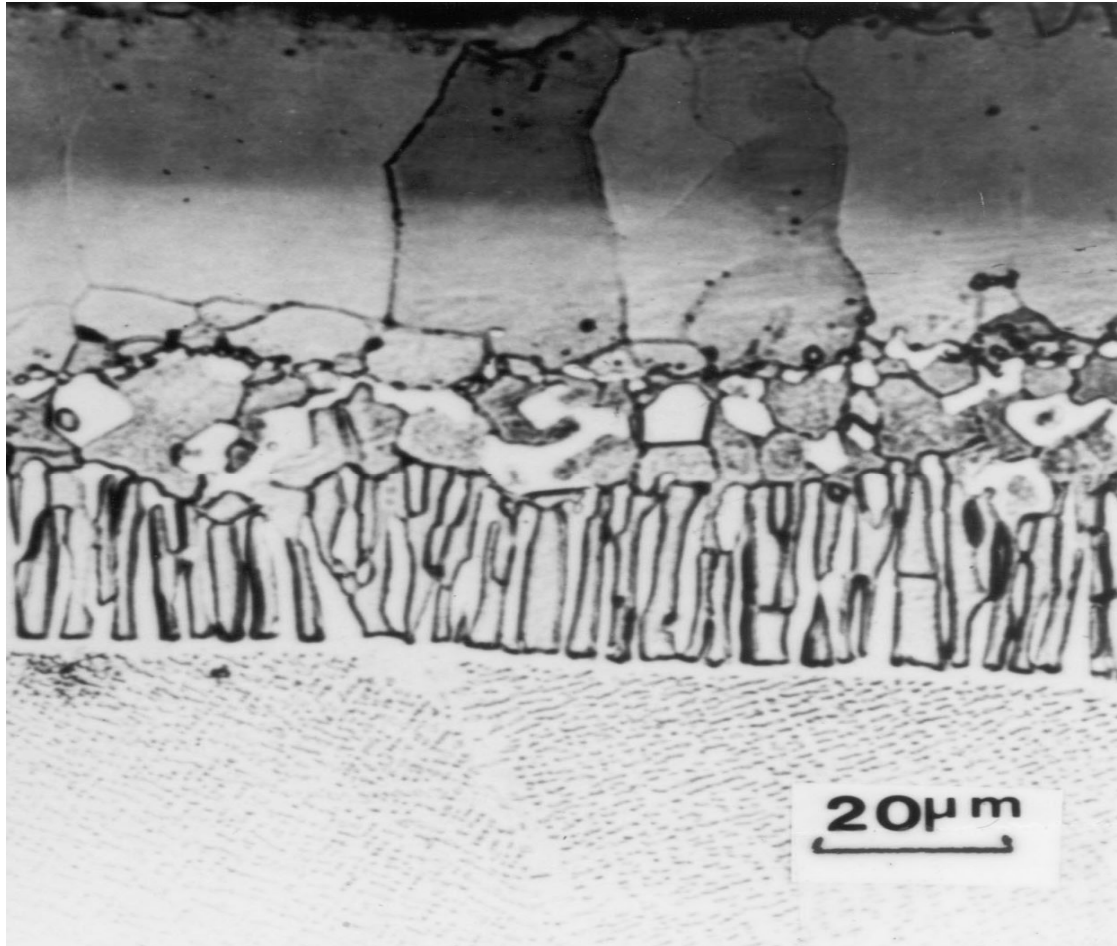


Ni-Al Phase Diagram

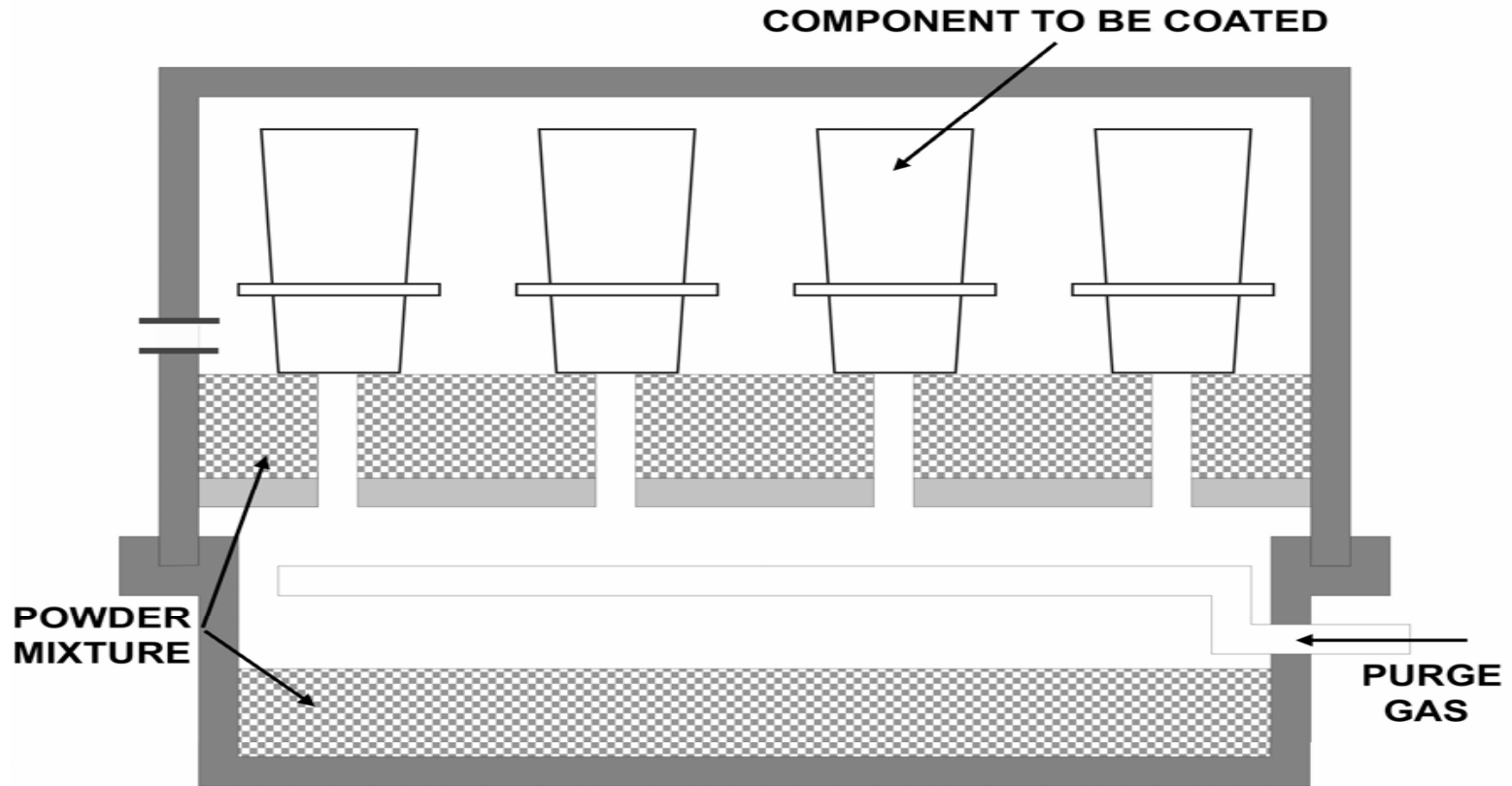




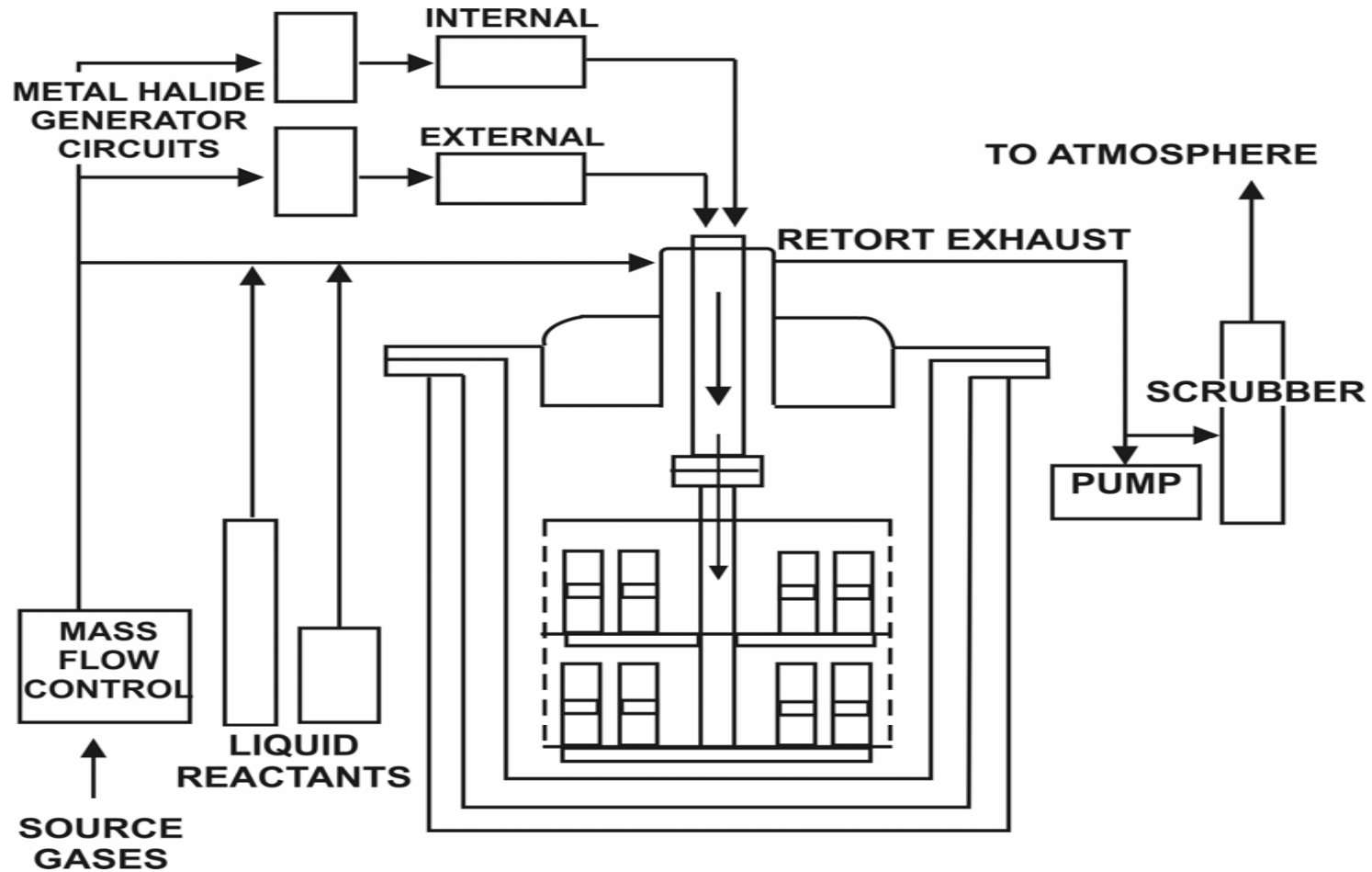
Cross-section of a High-Activity Diffusion Coating on a Ni-Base Superalloy



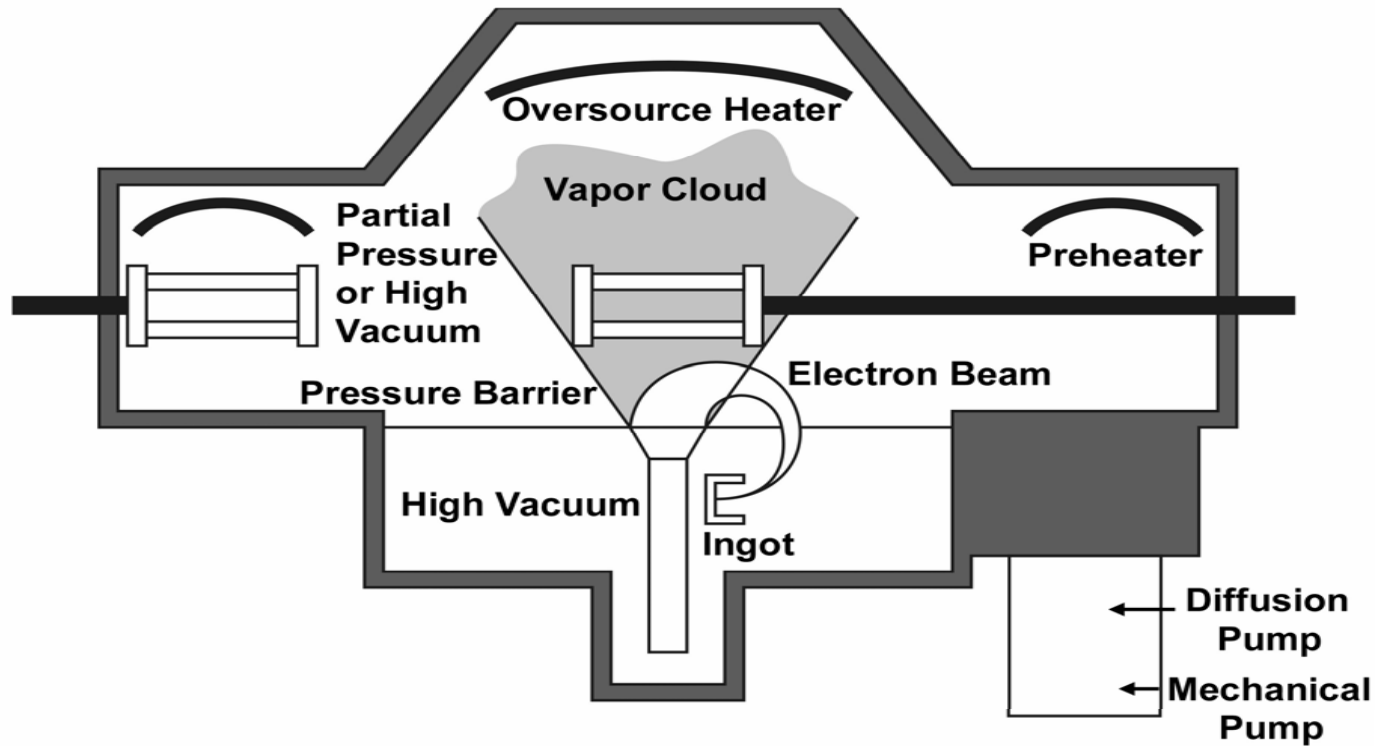
Cross-section of a Low-Activity Diffusion Coating on a Ni-Base Superalloy



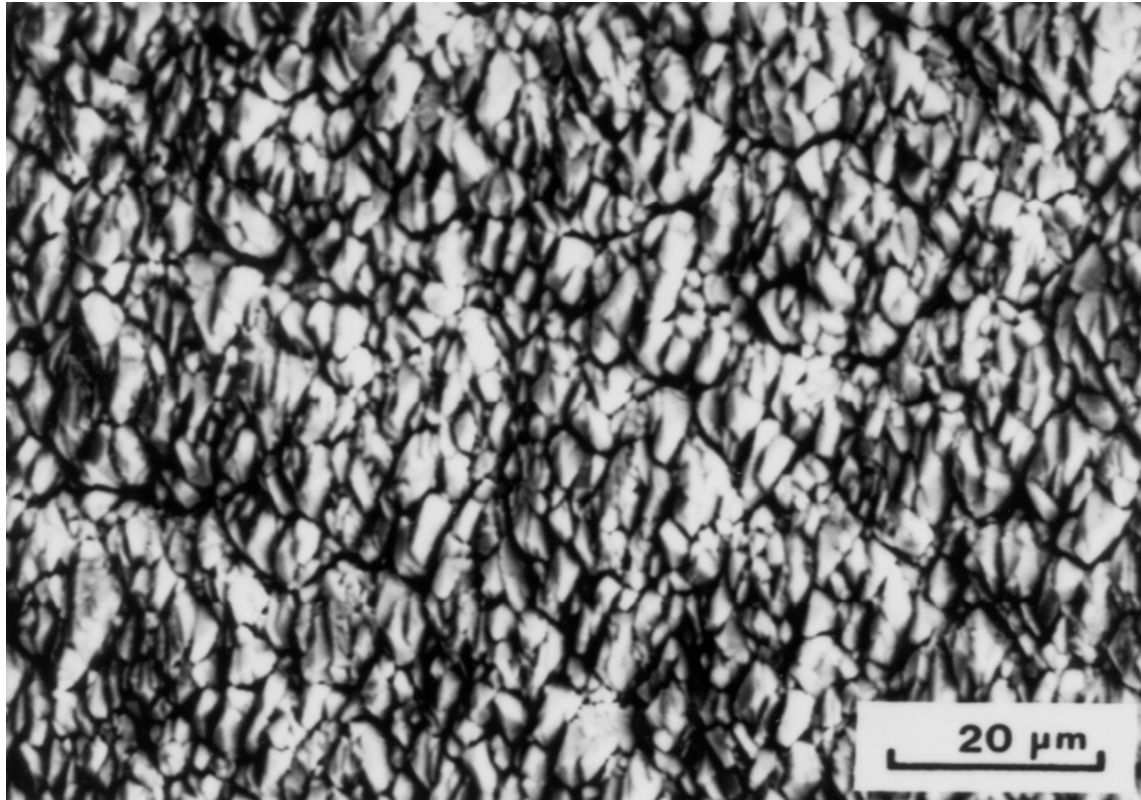
Schematic Diagram of an Above-the-Pack Coating Process



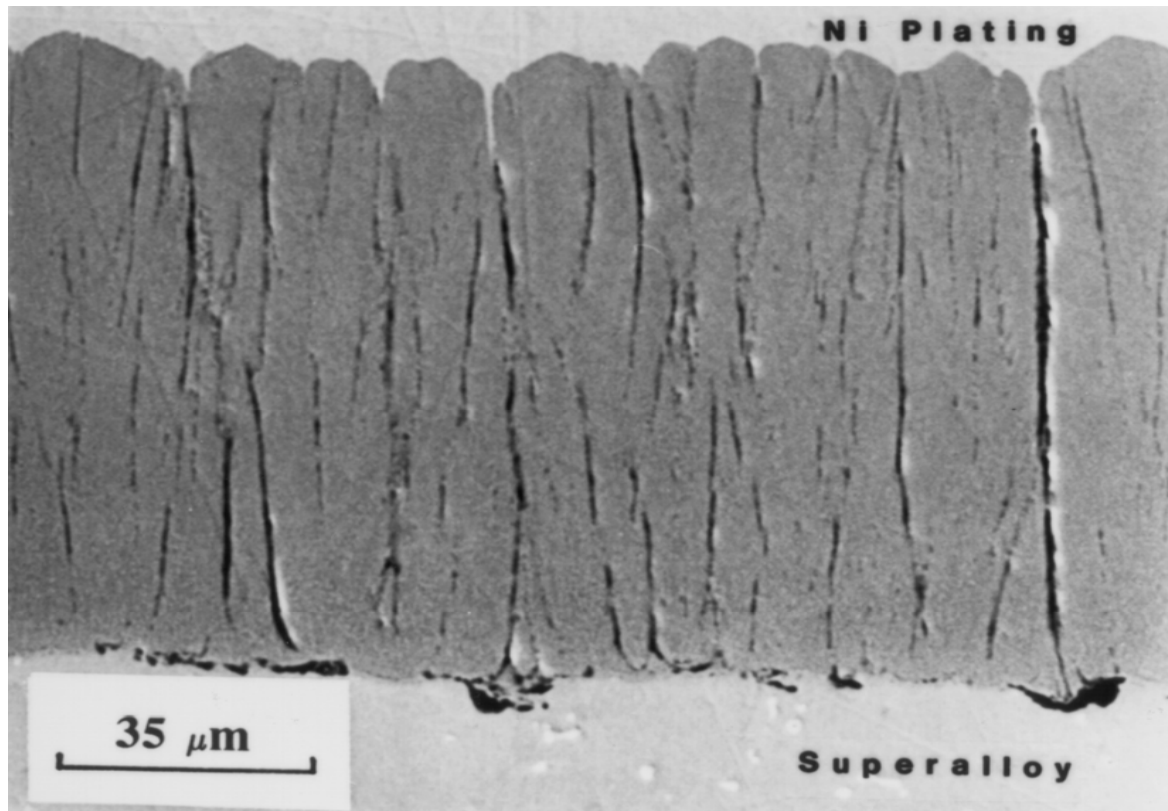
Schematic Diagram of a Chemical Vapor Deposition Process



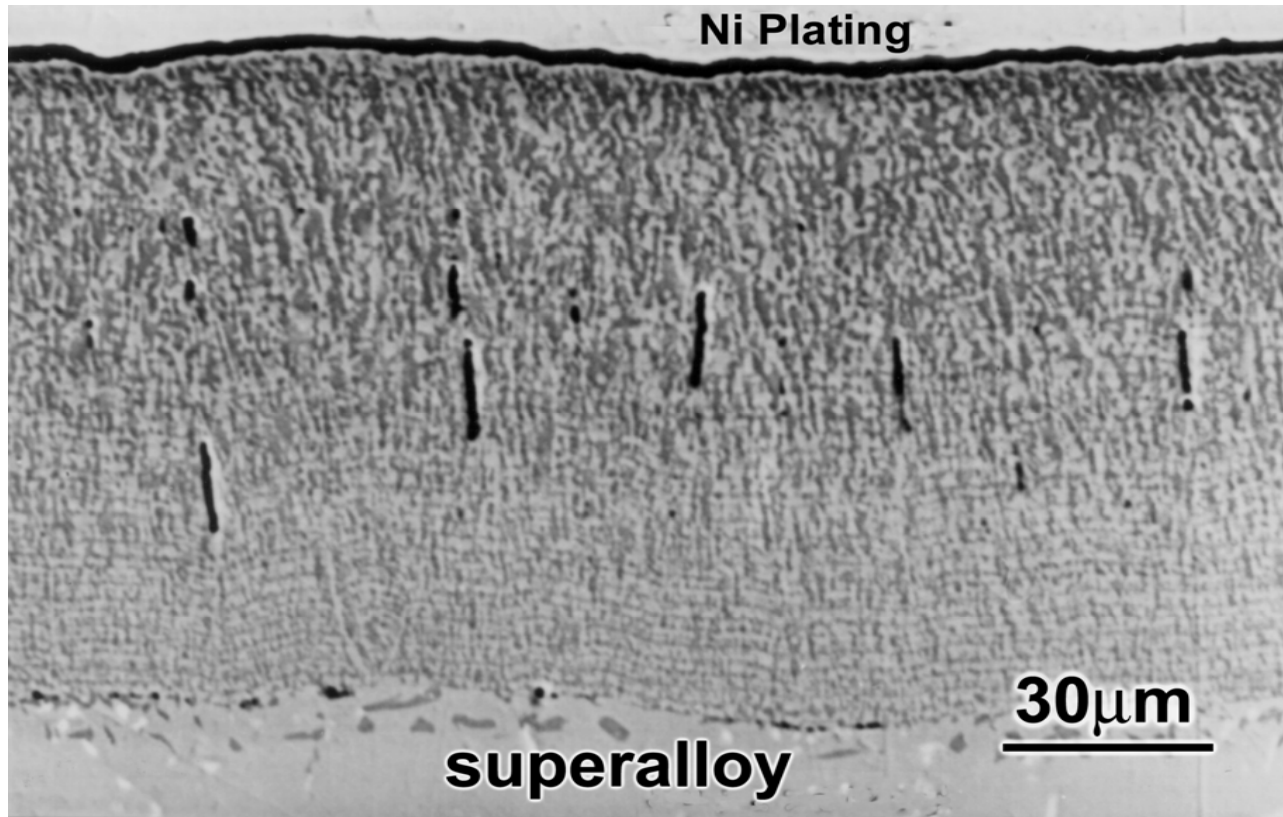
Schematic Diagram of an Electron Beam Physical Vapor Deposition (EBPVD) Process



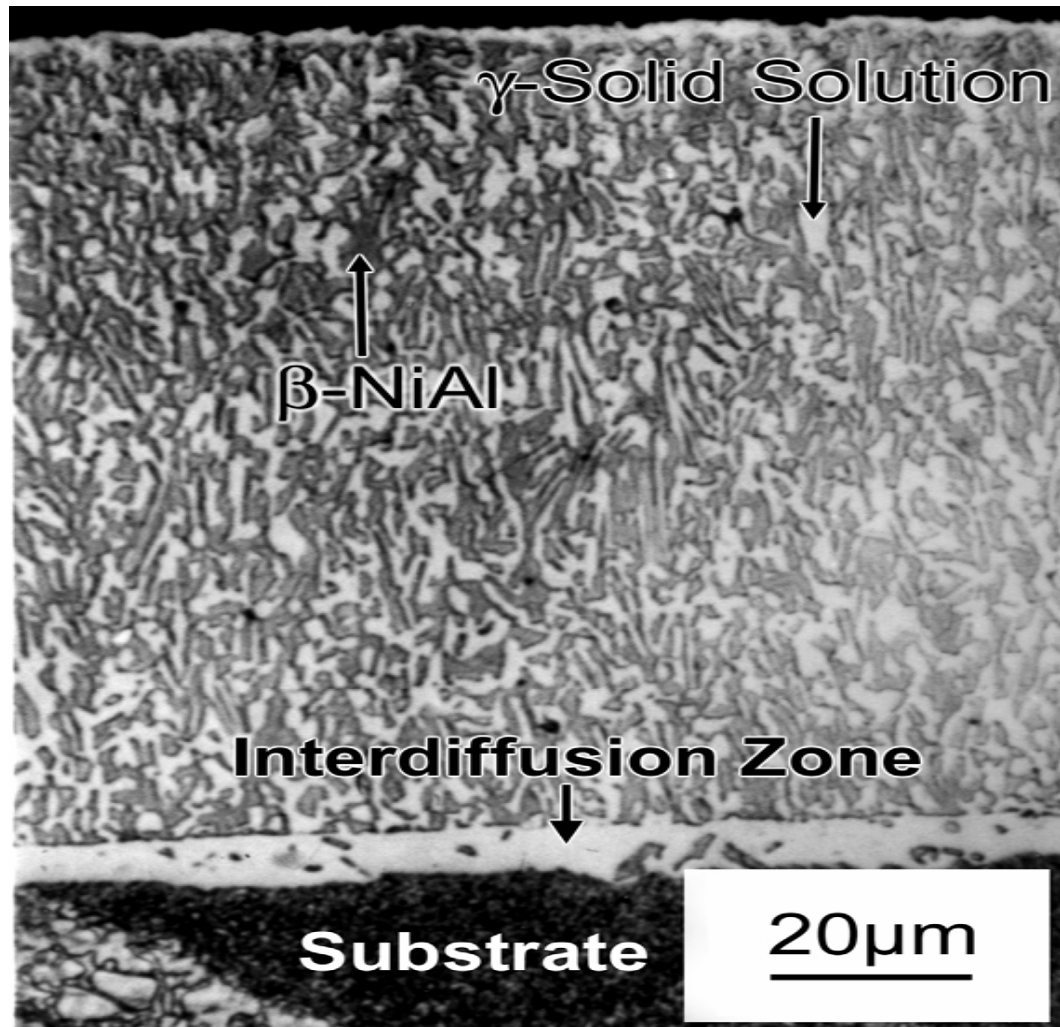
**Surface of an EBPVD CoCrAlY
Coating on IN738**



**Cross-section of the EB-PVD CoCrAlY
Coating from the previous slide**

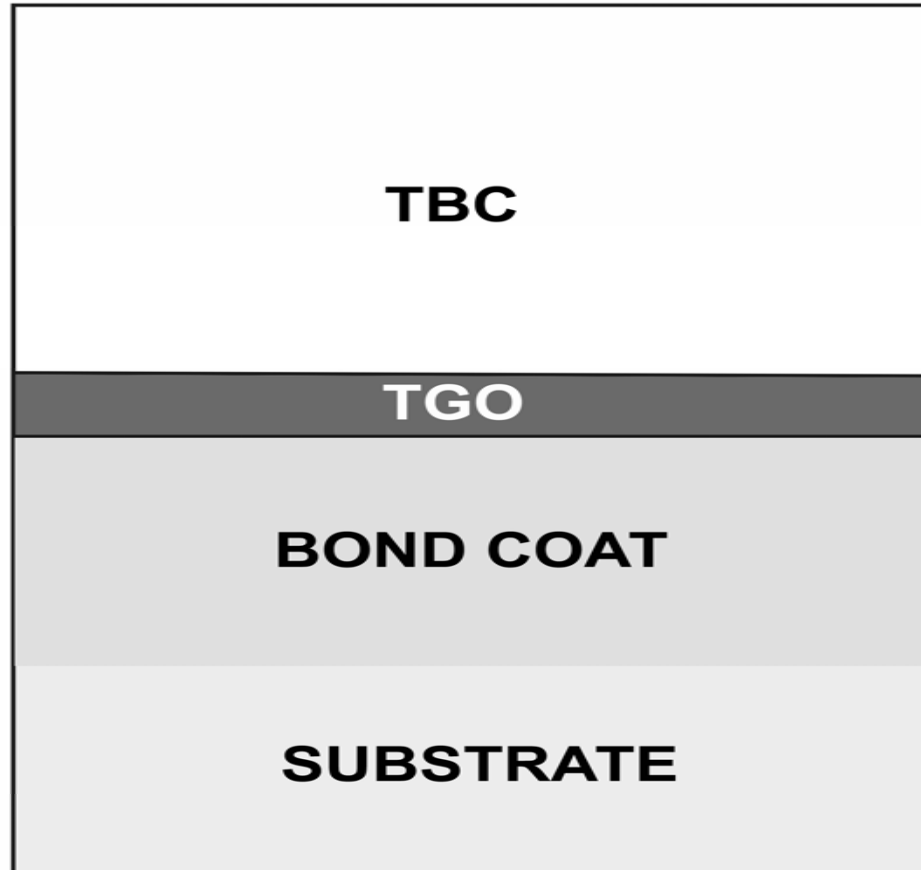


Cross-section of the EBPVD CoCrAlY Coating after Peening and Heat Treating

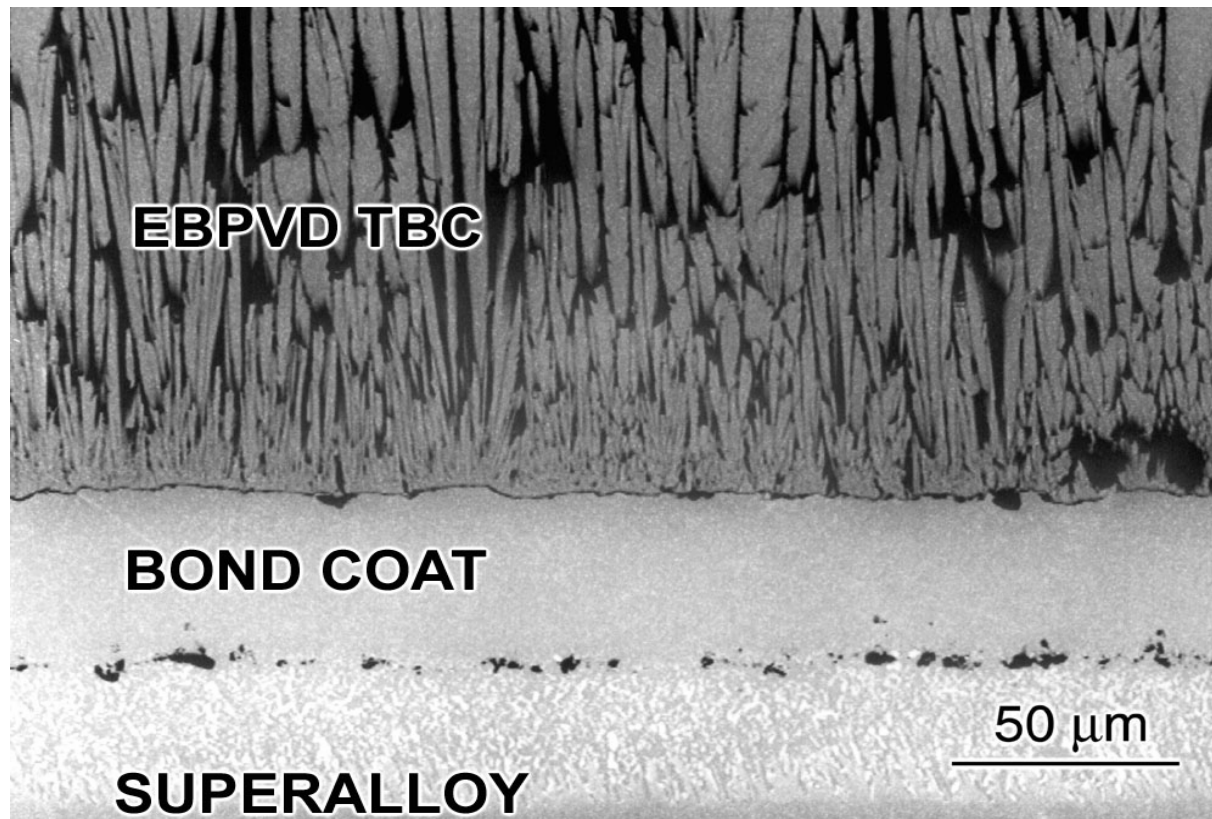


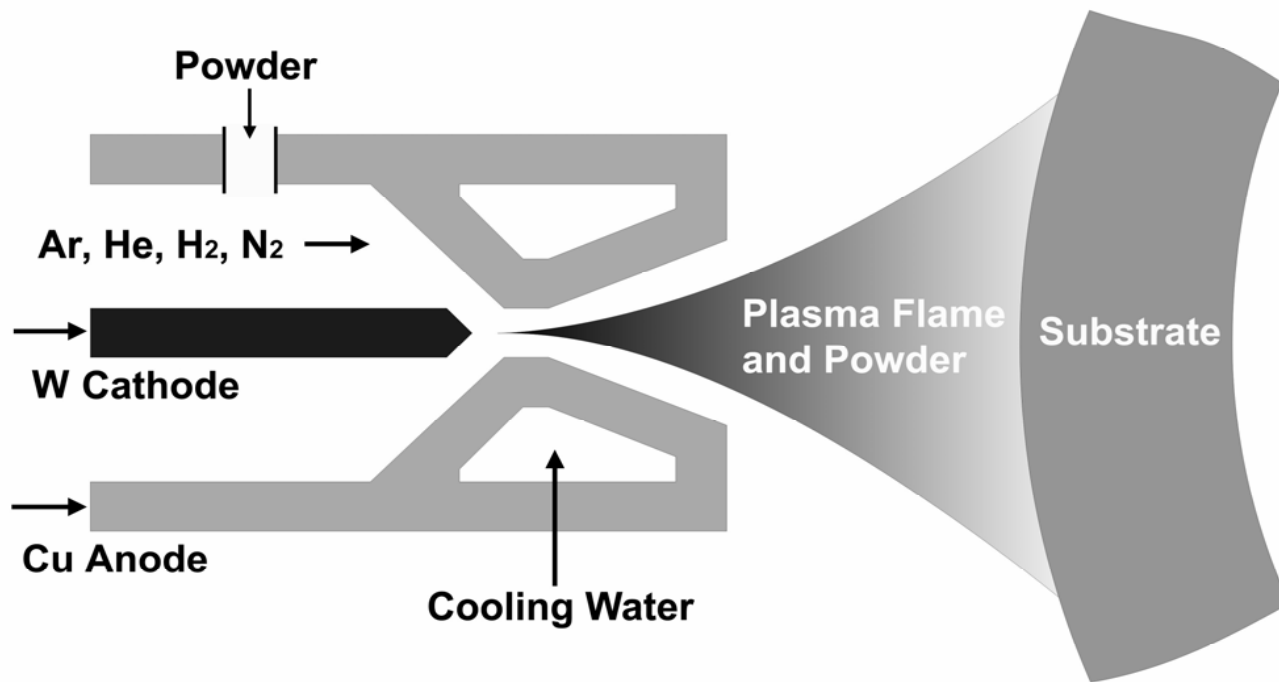
**Cross-section of an EBPVD
NiCrAlY Coating**

Schematic Diagram of a Thermal Barrier Coating (TBC)



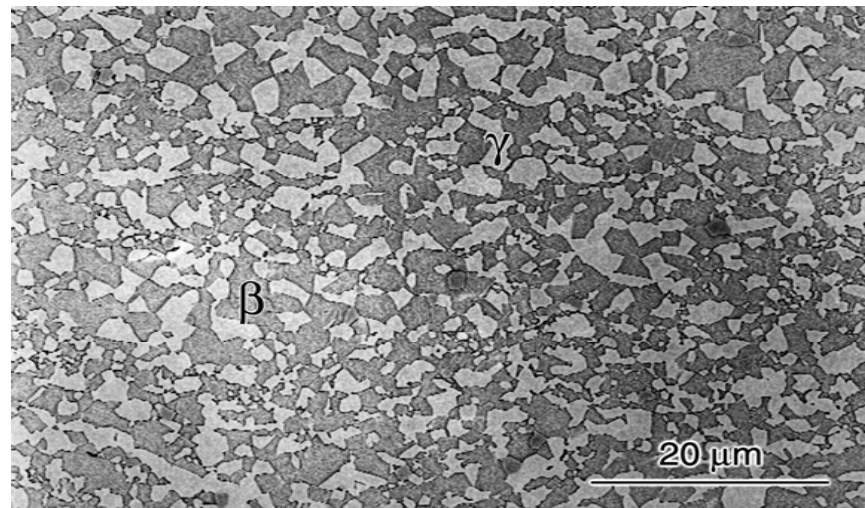
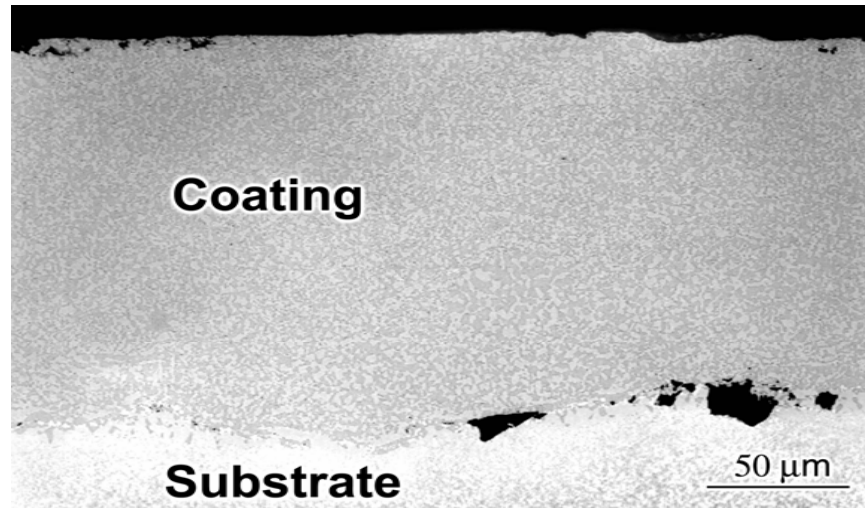
Cross-section of a TBC Deposited by EBPVD



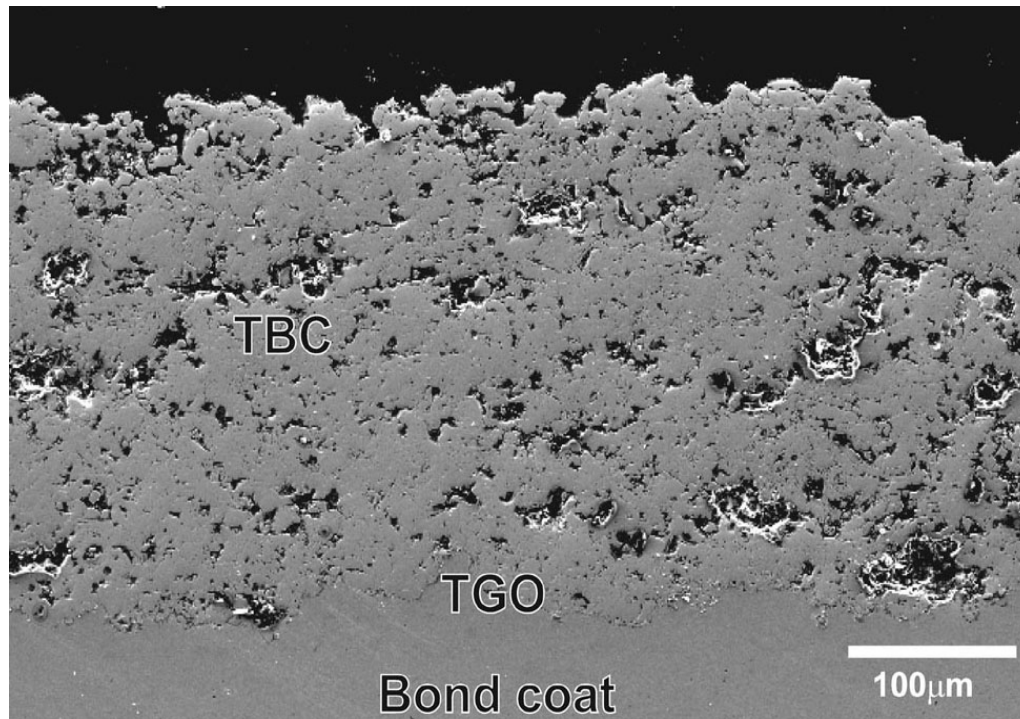


Schematic Diagram of a Plasma Deposition System

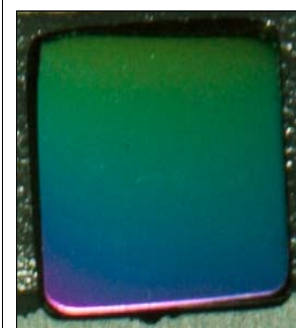
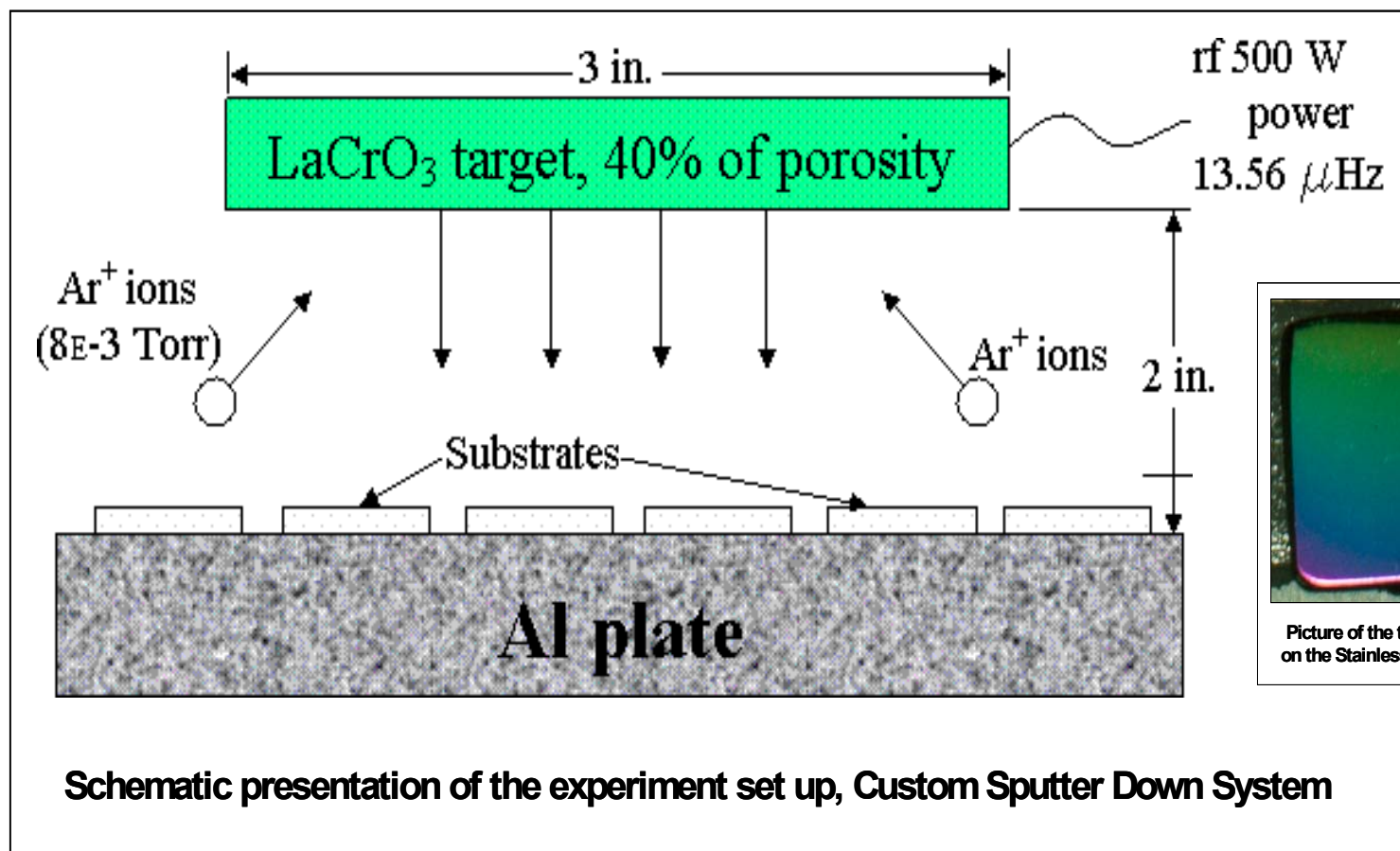
Cross-section of a NiCoCrAlY Coating Deposited by Argon-Shrouded Plasma Spraying



Cross-section of a TBC Deposited by Air Plasma Spraying (APS)



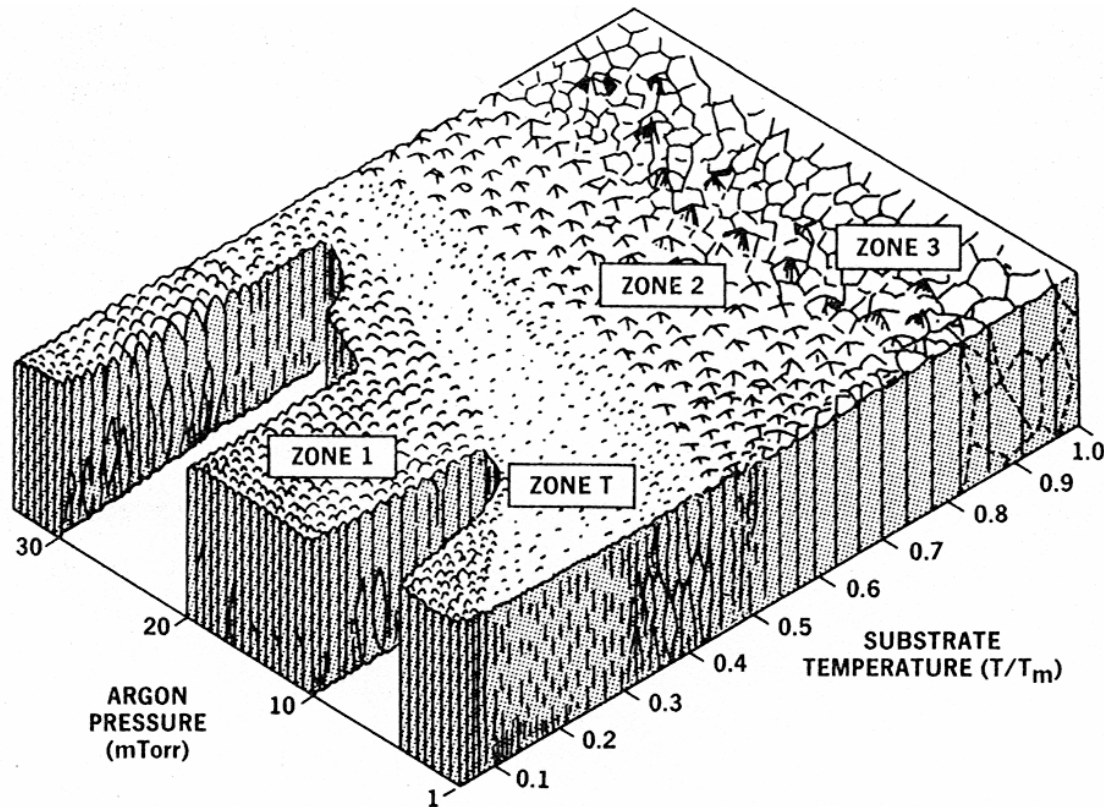
Magnetron Sputtering



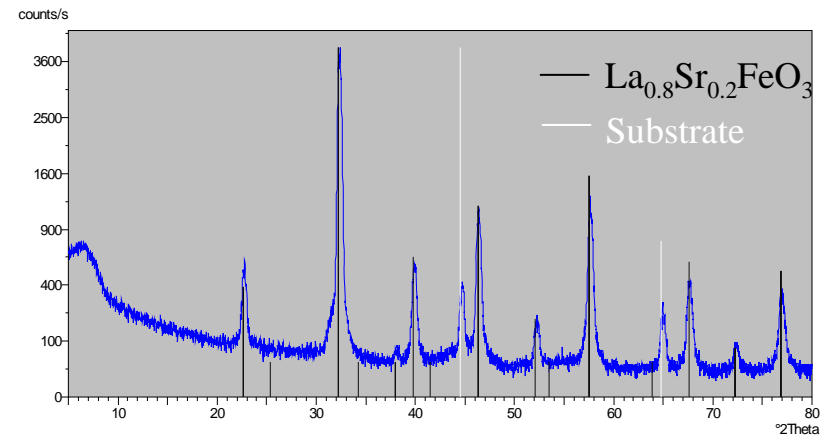
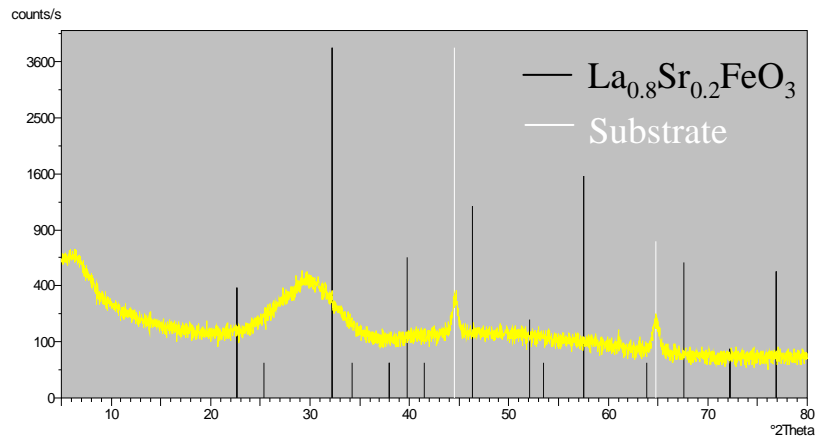
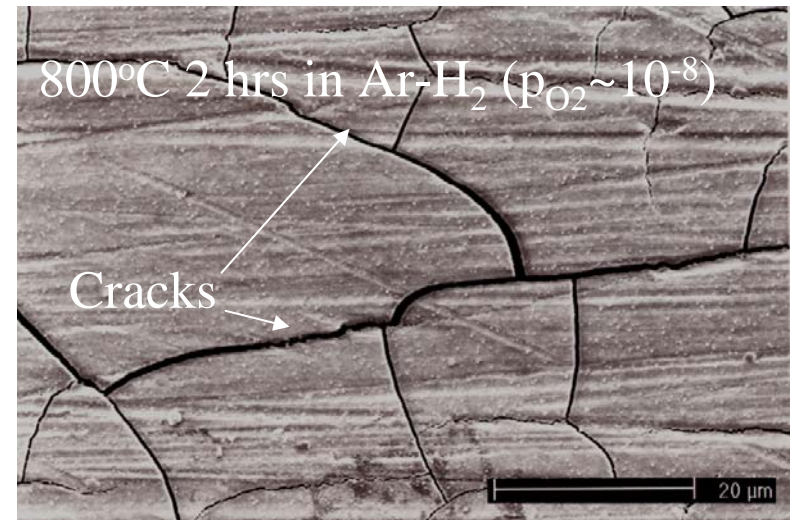
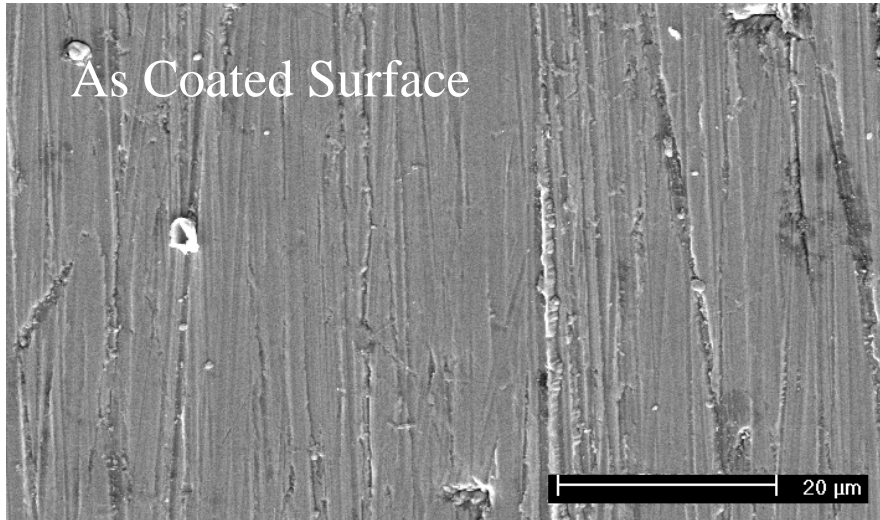
Picture of the thin film LaCrO₃ on the Stainless Steel Substrate

Perovskite target - LaCrO₃, hot pressed at 1400°C, green light color, 40% porosity;
 Substrates - Cr containing Stainless Steel; Substrate Temperature - 25°C;
 Pressure - 8x10⁻³ Torr Ar⁺; Deposition time - 5 hours.

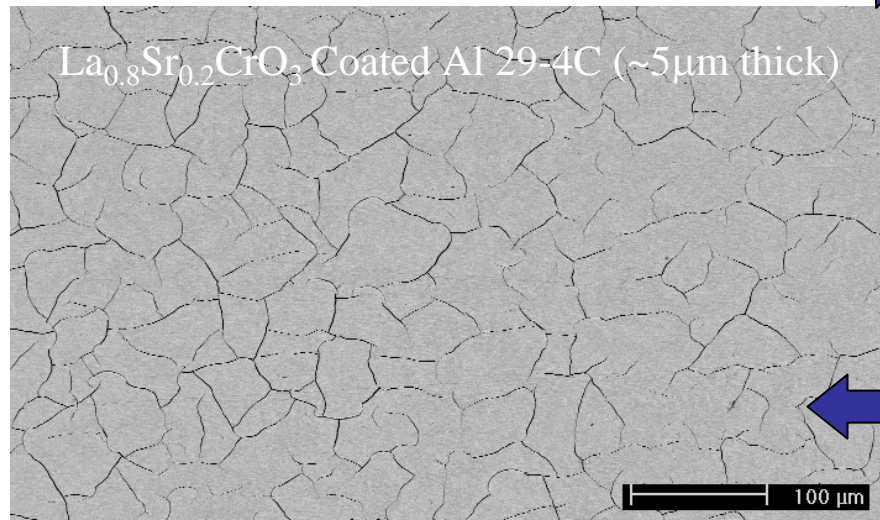
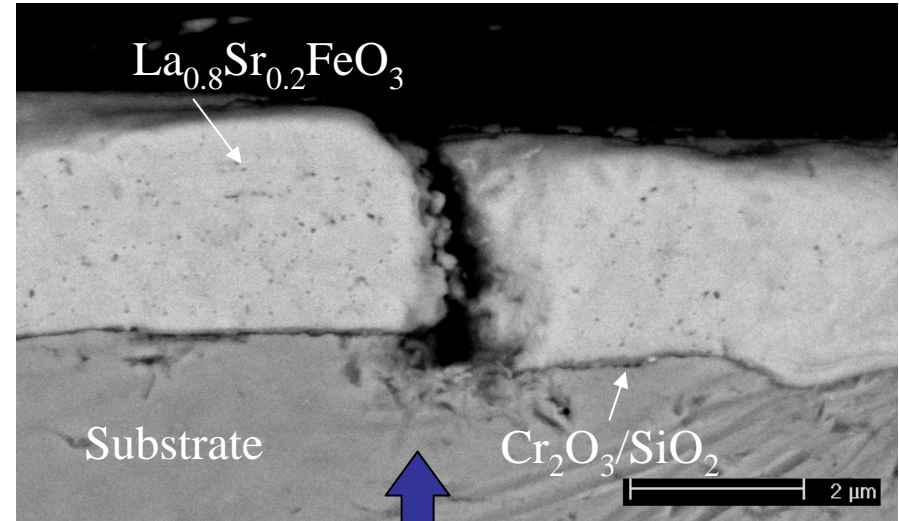
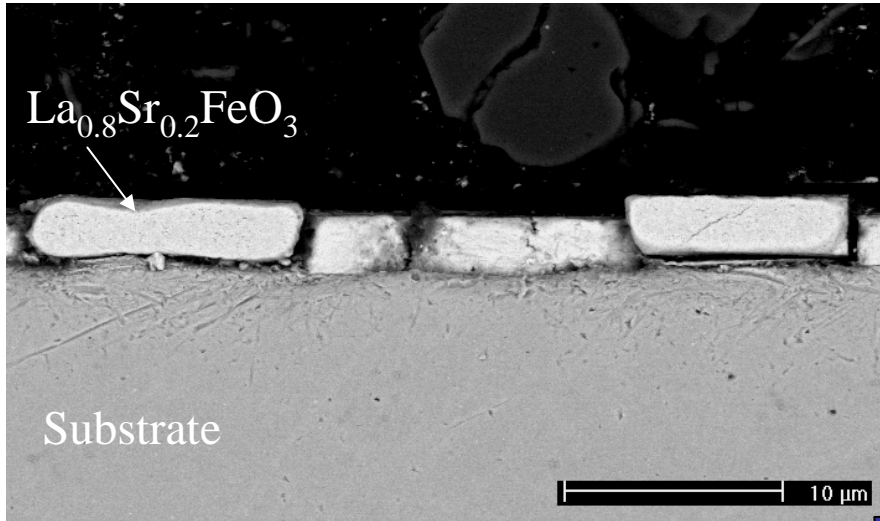
Effect of Deposition Conditions on the Microstructure of Sputtered Coatings



$\text{La}_{0.8}\text{Sr}_{0.2}\text{FeO}_3$ Coated E-Brite ($\sim 5\mu\text{m}$ thick)



$\text{La}_{0.8}\text{Sr}_{0.2}\text{FeO}_3$ Coated E-Brite ($\sim 5\mu\text{m}$ thick)

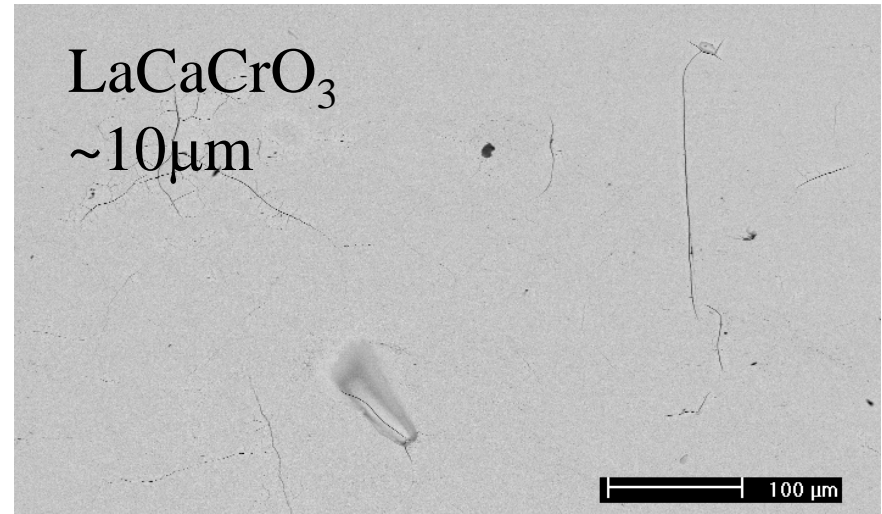
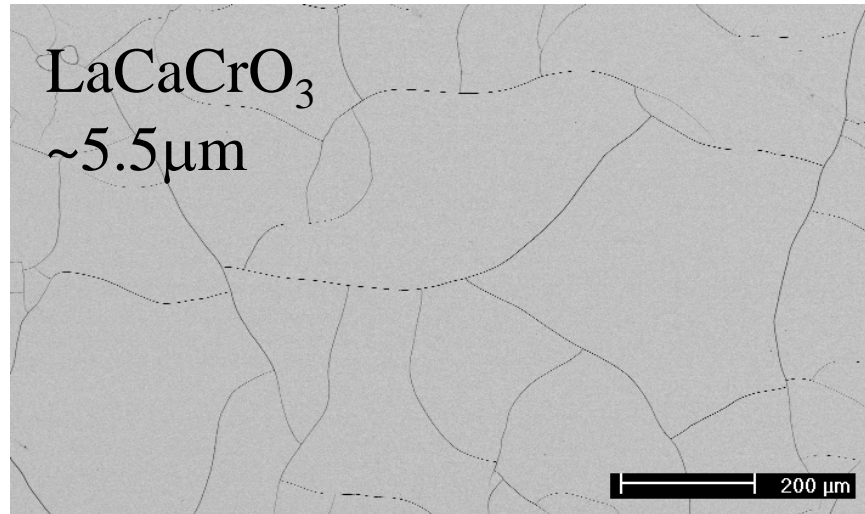
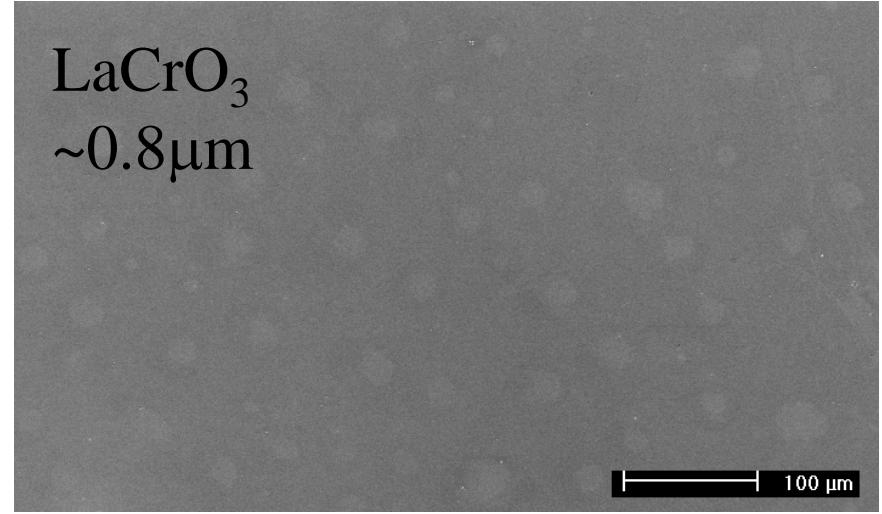
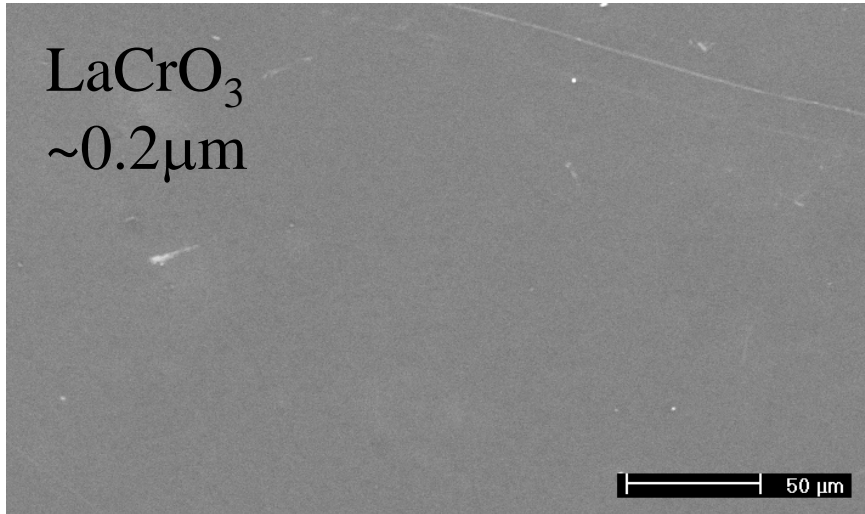


Cross sections show the coating to be much more dense, but also confirms the cracks seen from the surface

Chromite coating cracked as well after same exposure conditions

Various Thicknesses of LaCrO_3 Based Coatings

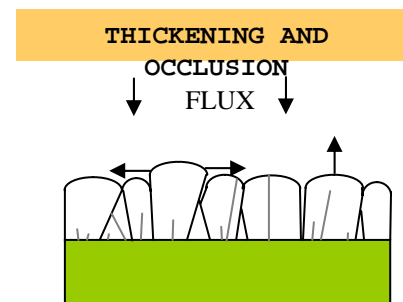
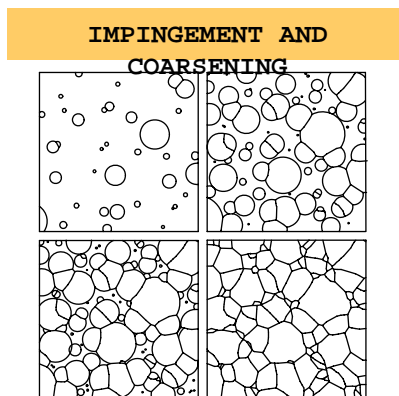
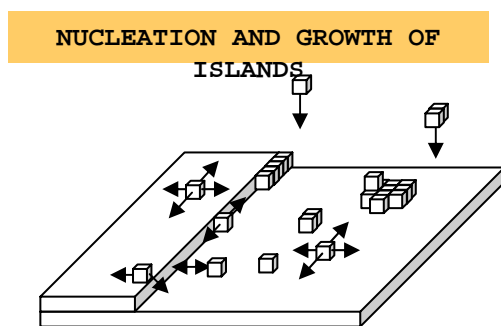
2hrs Ar- H_2 800°C





Pulsed Laser Deposition of lanthanum-based oxides

Dr. John P. Leonard, Materials Science and Engineering, University of Pittsburgh, Pittsburgh PA



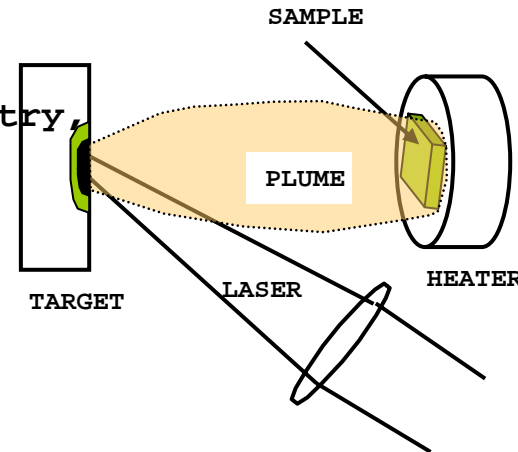
PROJECTS

- Pulsed laser deposition of LaCrO_3 films on YSZ, CeO_2 , multilayers
- Development of laser co-ablation technique for incorporation of Sr and other dopants into LaCrO_3
- La_2O_3 polycrystalline film formation on Si(001) and SiO_2 substrates, early stages of nucleation and growth

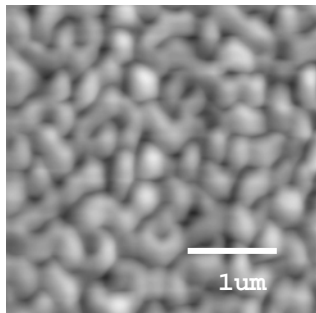
PULSED LASER DEPOSITION

- E = 10 to 150 eV
- PULSED FLUX
- NON STEADY-STATE ADATOM CONCENTRATIONS

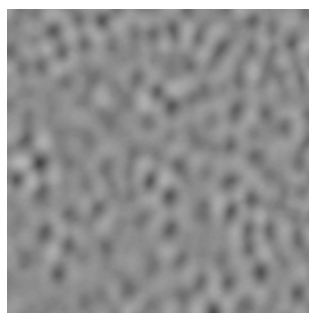
- Laser ablates material from target, forming a high-temperature vapor plume incident on sample.
- Congruent evaporation, complex stoichiometry, preferred technique for metal oxide deposition
- Tight control of submonolayer thicknesses
- Plume/chemical effects
 - Reactive processing in background gas
 - Energetic effects at film surface
- PLD has characteristics similar to 'energetic' MBE processes for improved epitaxial growth



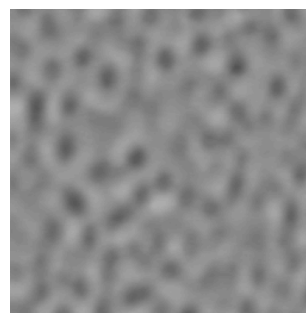
PLD 90°C



PLD 150°C



PLD 200°C



*Germanium (001)
homoepitaxy via PLD
With mound formation
via kinetic and step
bunching processes
(J.P. Leonard et al. 2002)*

$$h_{\text{rms}} = 60.9\text{\AA} \quad h_{\text{pv}} = 397\text{\AA} \quad h_{\text{rms}} = 28.2\text{\AA} \quad h_{\text{pv}} = 277\text{\AA} \quad h_{\text{rms}} = 24.5\text{\AA} \quad h_{\text{pv}} = 178\text{\AA}$$

Ba_2RuO_4
 $(\text{Ba,Ca})\text{CuO}_2$
 BaFeO_{19}
 $\text{Ba}(\text{Sr,Ti})\text{O}_3$
 Bi_2VO_5
 $\text{Bi}_3\text{Fe}_5\text{O}_{12}$
 CdWO_4
 CeO_2
 $(\text{Sr,Ti})\text{O}_3$
 Co_3O_4
 CuO_2
 Fe_2O_3
 GeO_2
 HfO_2
 LaAlO_3
 LaNiO_3
 LiNbO_3
 MgO
 MgZnO
 $\text{Na}_4\text{Zr}_2(\text{SiO}_4)_3$
 $(\text{Ni,Co,Zn})\text{Fe}_2\text{O}_4$
 $(\text{Pb,Lu})(\text{Zr,Ti})\text{O}_3$
 RuO_2
 Ta_2O_5
 V_2O_5
 $\text{Y}_3\text{Al}_5\text{O}_{12}$
 $\text{Y}_3\text{Fe}_5\text{O}_{12}$

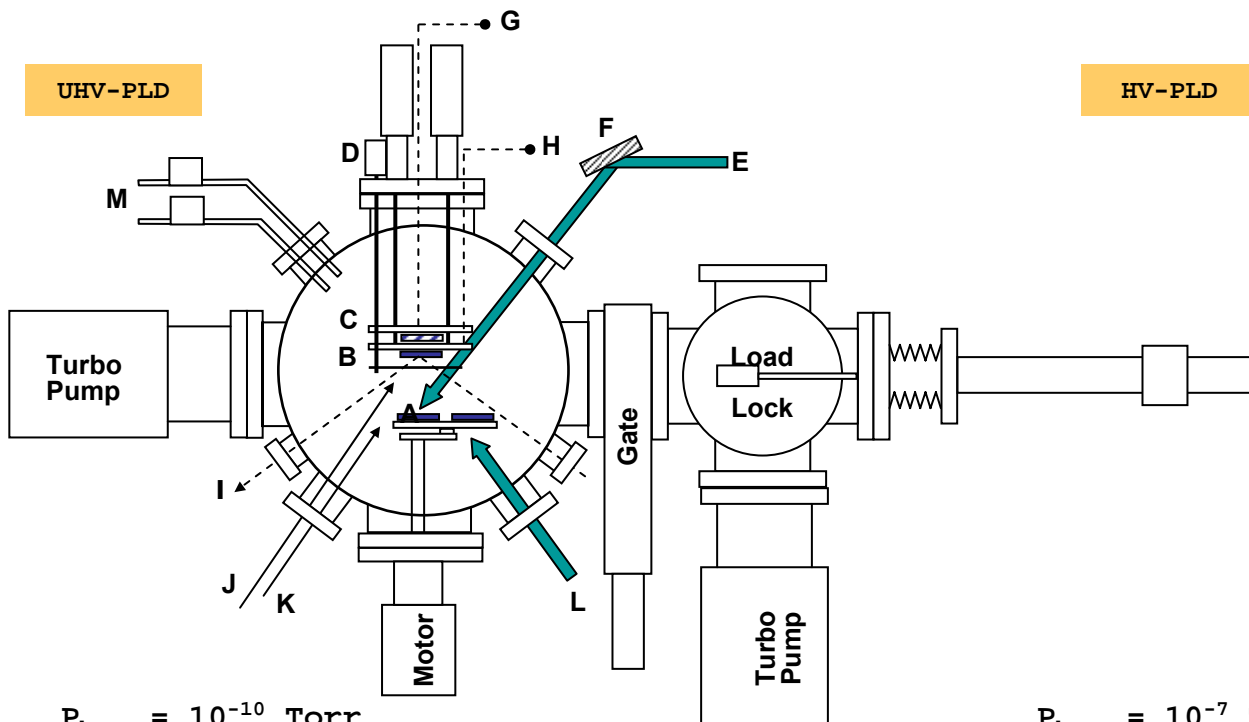
*Some oxide
systems
that have been
successfully
deposited
worldwide*

with PLD

Equipment

- We have developed two PLD systems that incorporate critical features necessary for fundamental studies and production of high-quality oxide films.

UHV-PLD



$P_{\text{base}} = 10^{-10}$ Torr

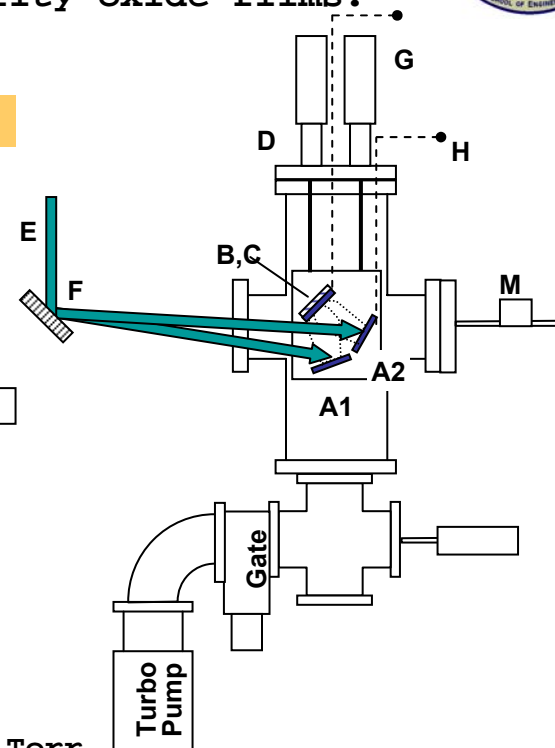
$P_{\text{Gas}} = 0-500$ mTorr, 2-channel

$T_{\text{substrate}} = 20 - 1000^\circ\text{C}$

Targets = (4) 10-50mm dia, 4-position carousel

- (A) Target
- (B) Substrate
- (C) Heater (radiative, backside)
- (D) Shutter
- (E) Laser beam, (KrF 248nm 30ns)
- (F) rastering mirror

HV-PLD



$P_{\text{base}} = 10^{-7}$ Torr

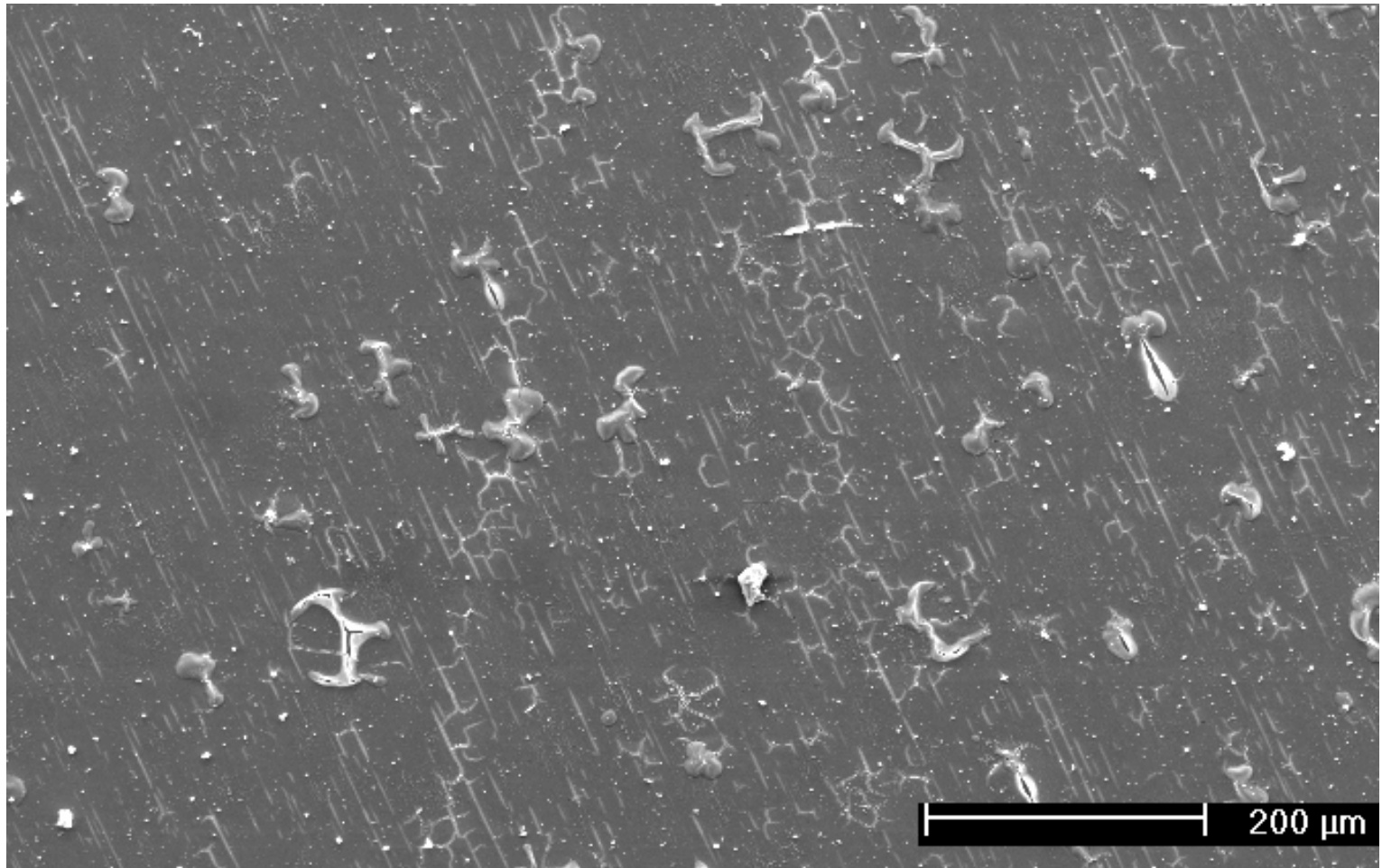
$P_{\text{Gas}} = 0-500$ mTorr, 1-channel

$T_{\text{substrate}} = 20 - 500^\circ\text{C}$

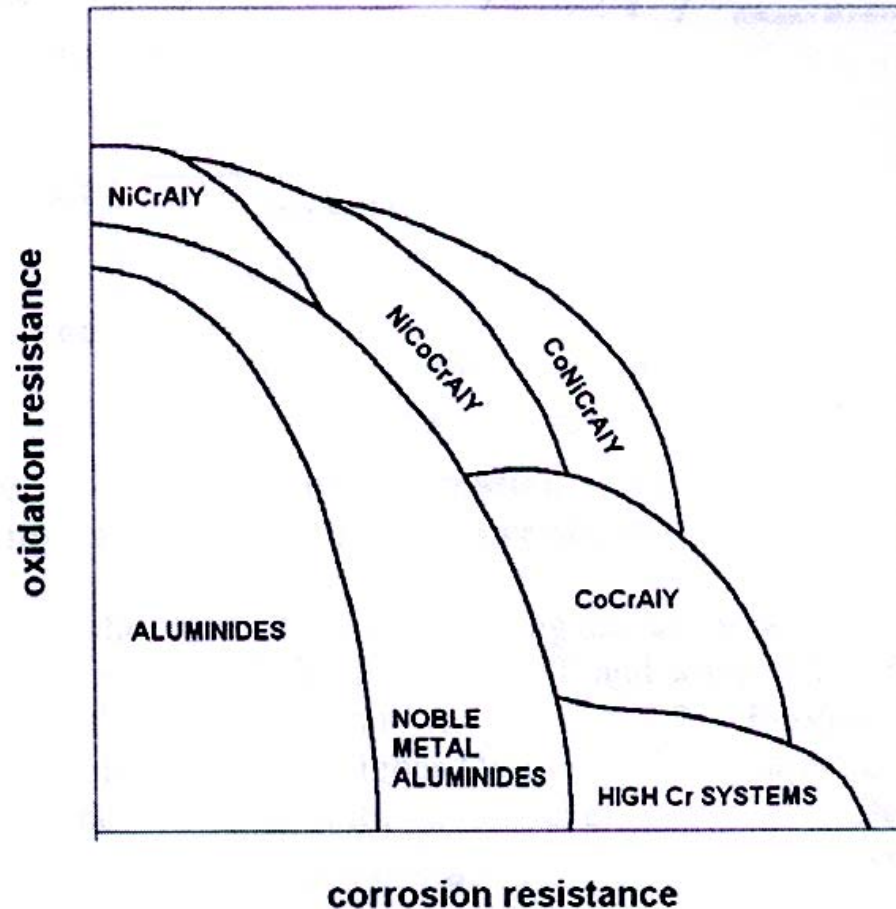
Targets = (2) 10-25mm dia, co-ablation

- (G) Thermocouple
- (H) Ion probe circuit (flux monitor)
- (I) Reflectance spectroscopy
- (J) Infrared pyrometry
- (K) UV lamp irradiation
- (L) Post-deposition laser melting

PLD-SrO Coated Ni

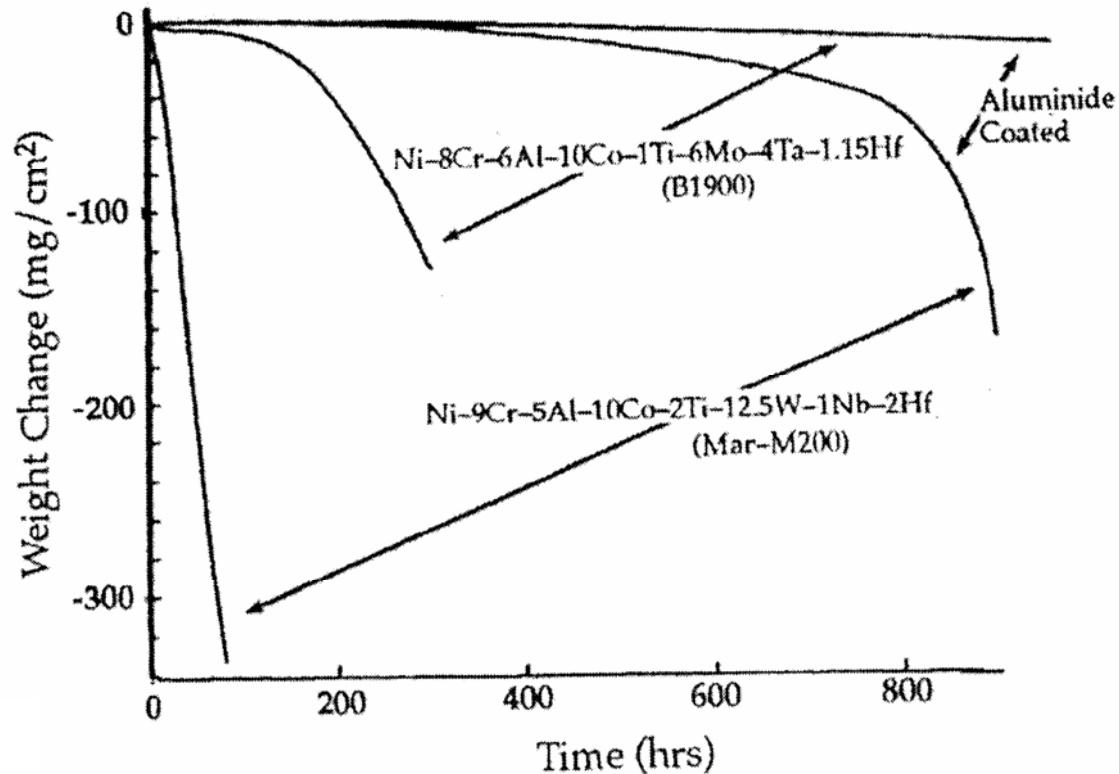


Coating Durability Limitations

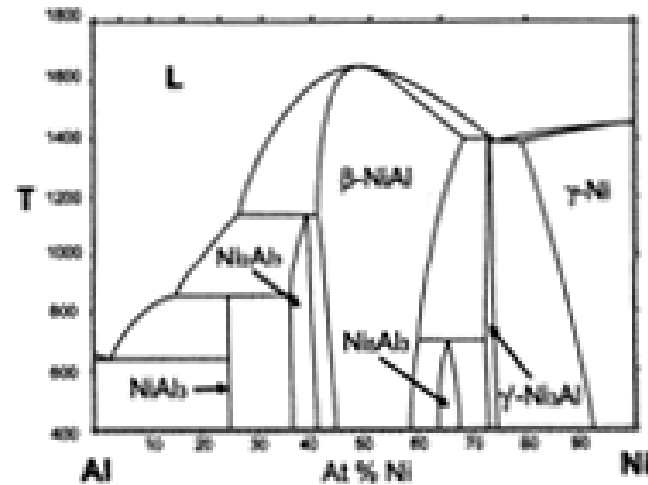


Effect of composition on the hot corrosion and oxidation resistance of overlay and diffusion aluminide coatings

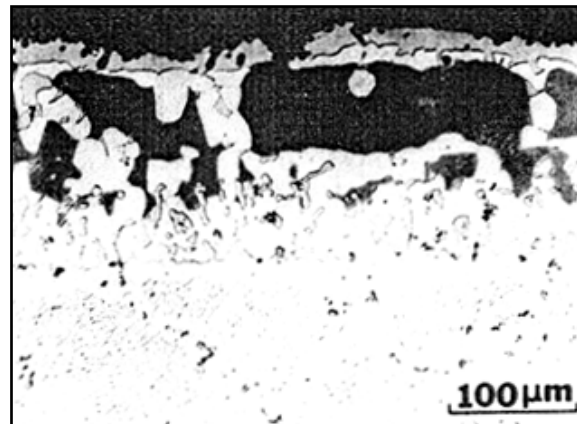
The Oxidation Degradation Process for Aluminide Coatings



The oxidation Degradation Process for Aluminide Coatings

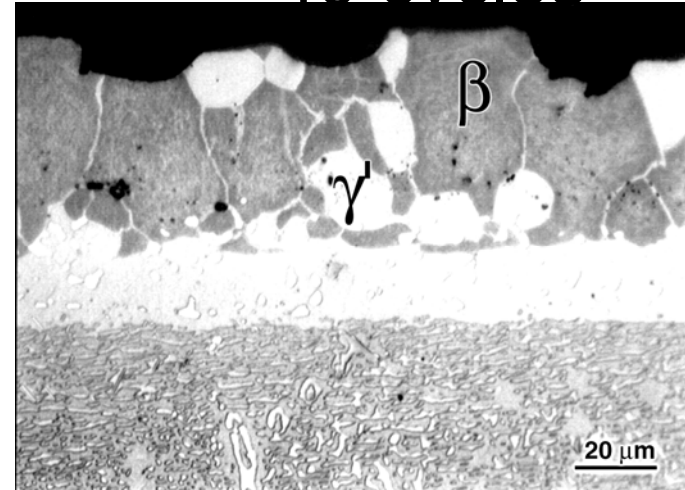
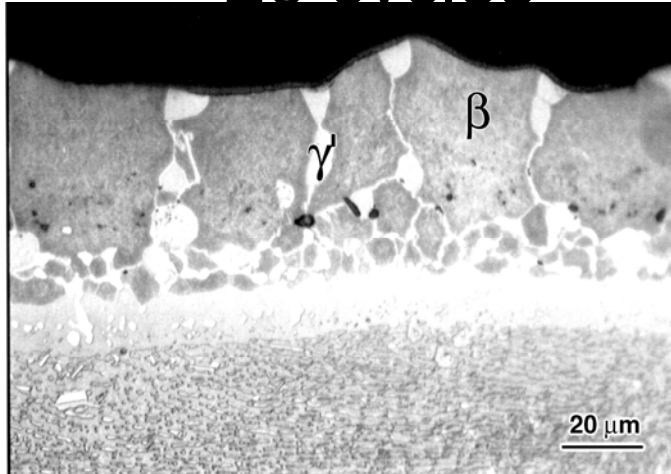


10-2

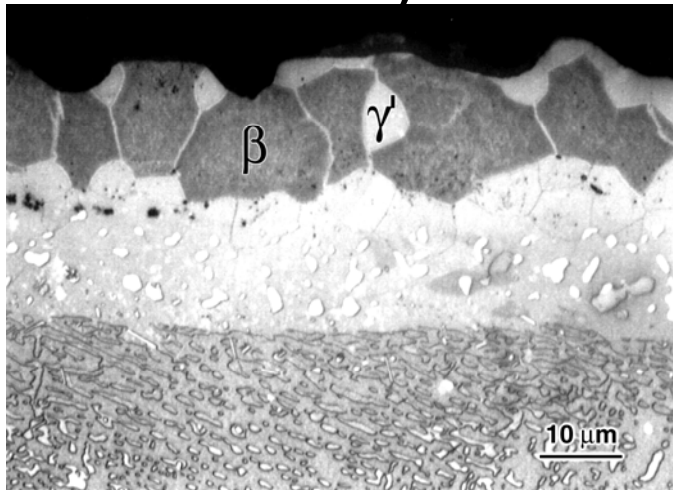


The Oxidation Degradation Process for Aluminide Coatings

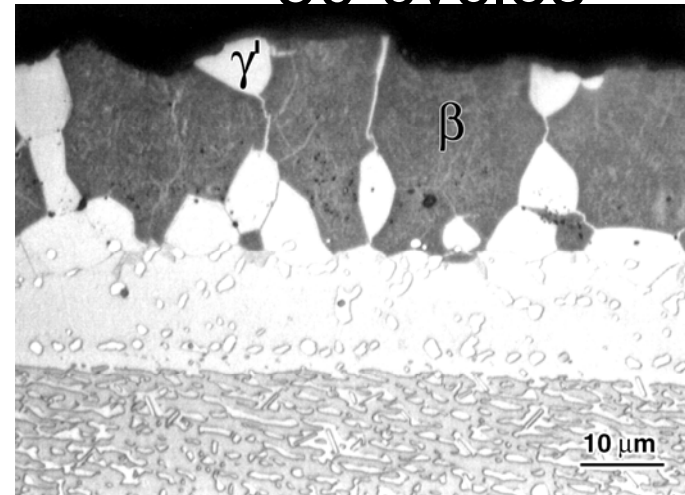
20 cycles 1200 °C 40 cycles



60 cycles



80 cycles

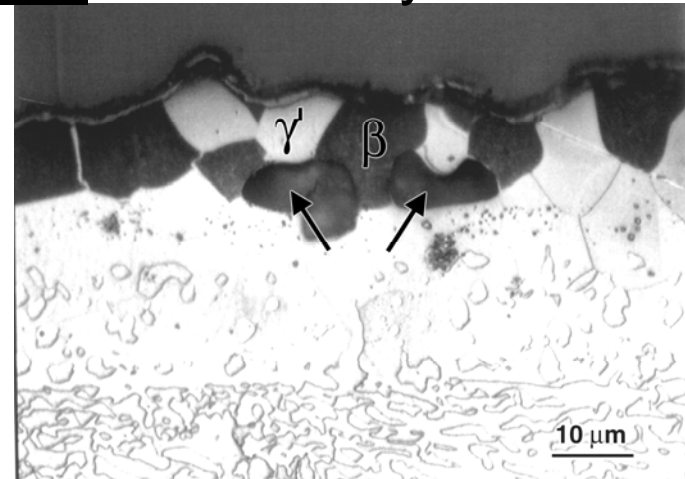
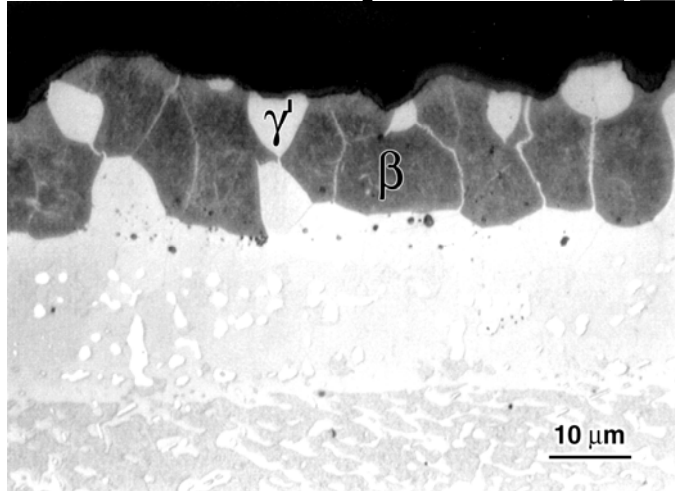


PLATINUM ALUMINIDE BOND COAT

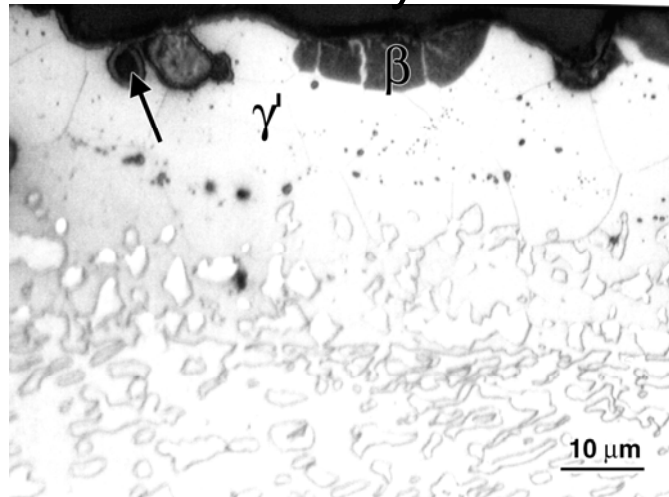
100 cycles

1200 °C

130 cycles

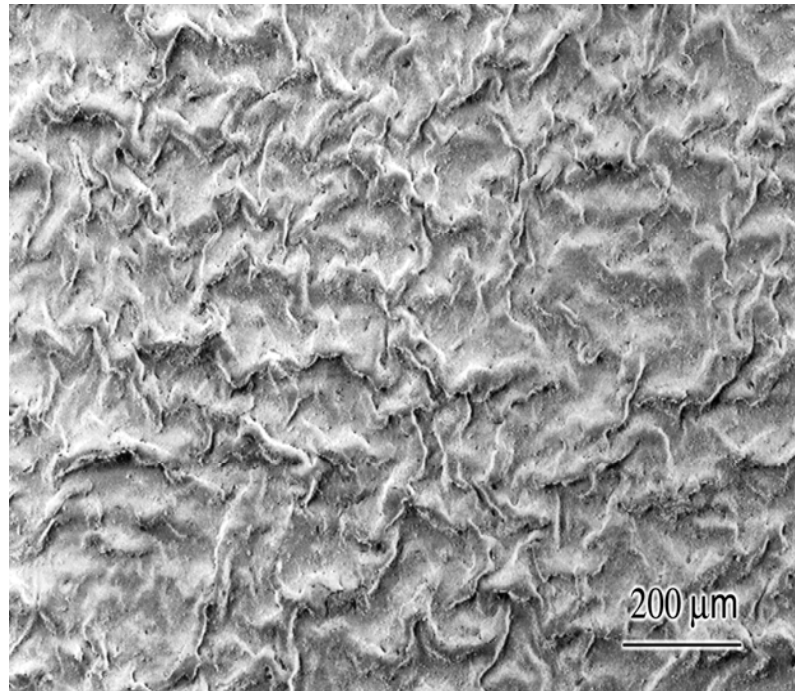


200 cycles



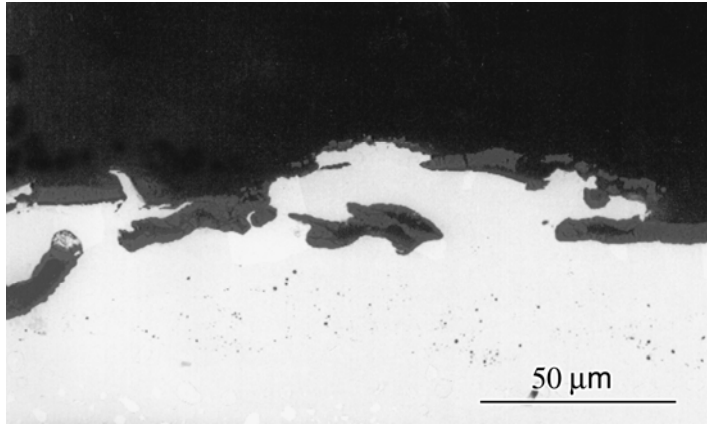
PLATINUM ALUMINIDE

Exposure at 1100 °C for 955 cycles

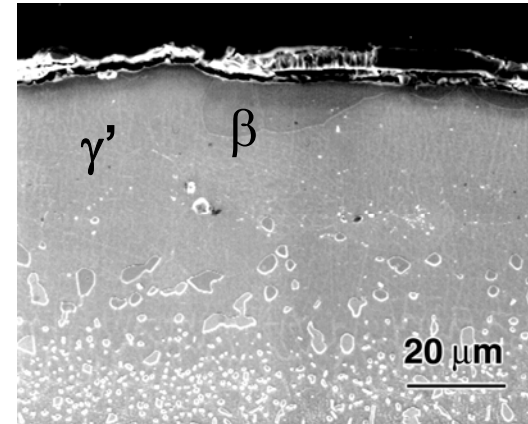


Platinum Aluminide Bond Coat Cyclic Oxidation in Air at 1100°C

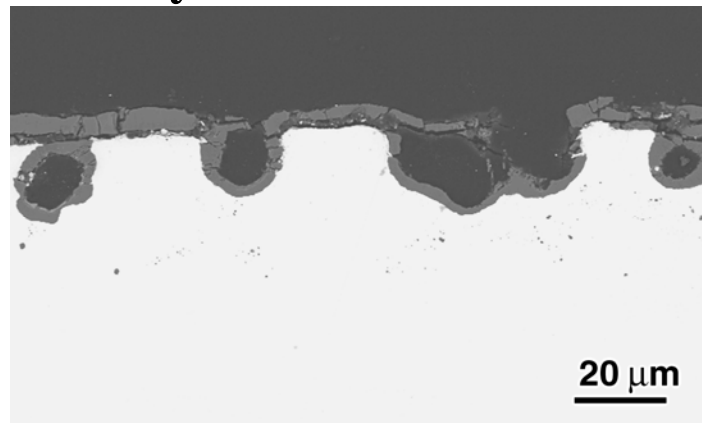
955 cycles



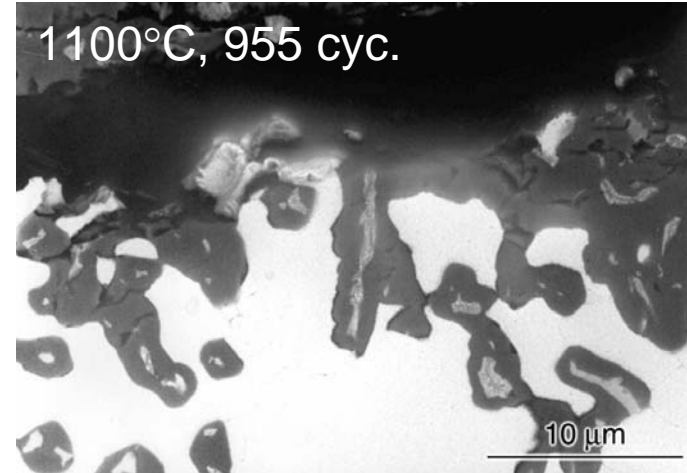
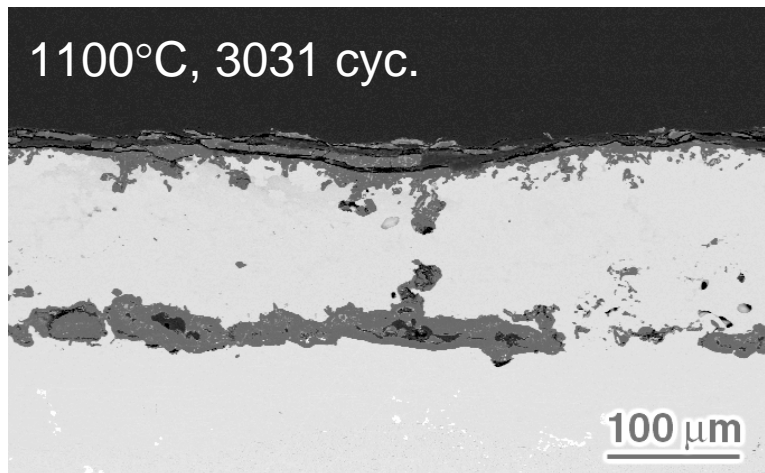
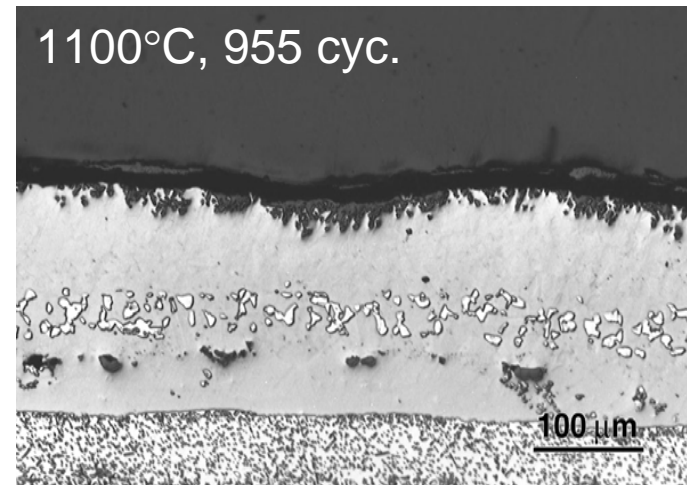
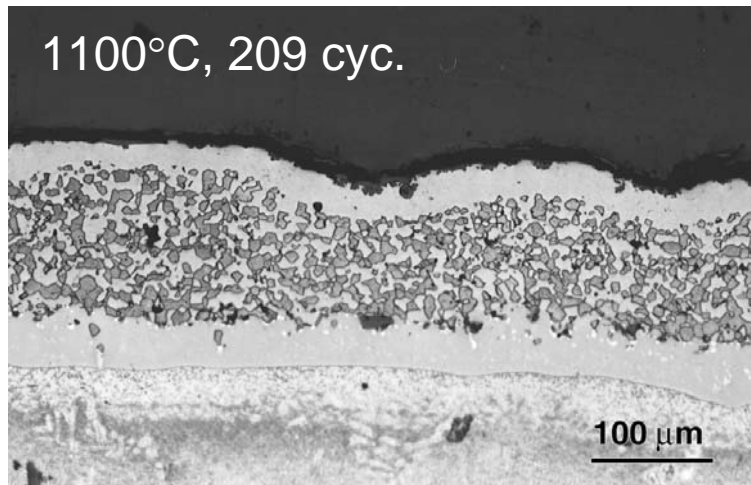
955 cycles



3031 cycles

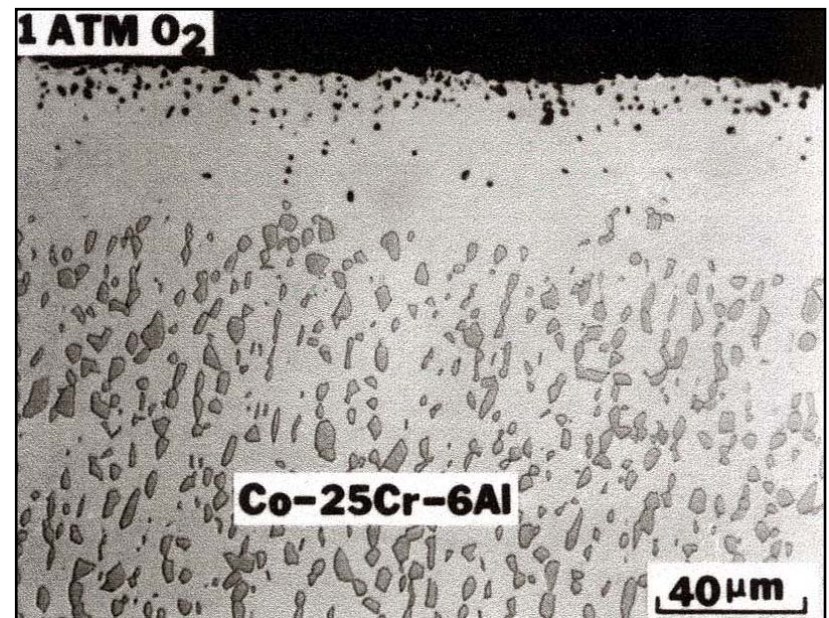
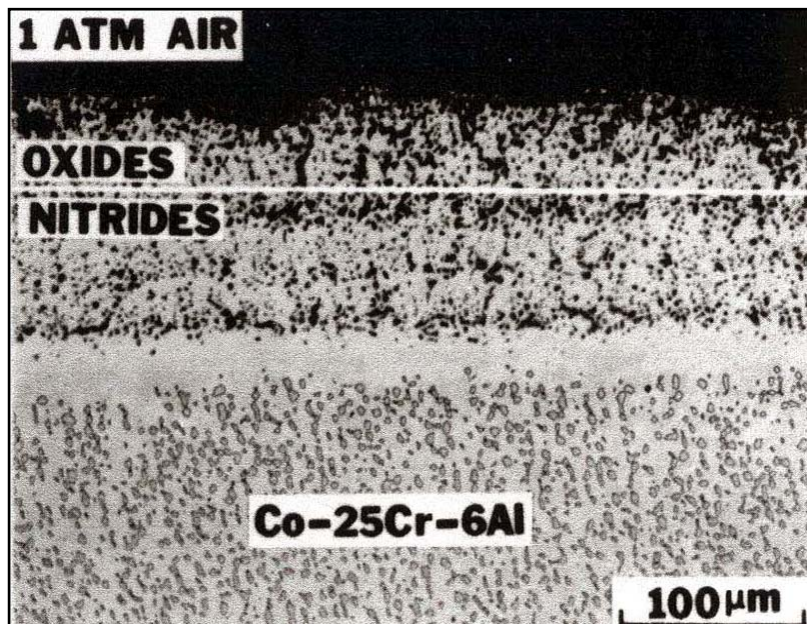


The oxidation Degradation of NiCoCrAlY Coatings

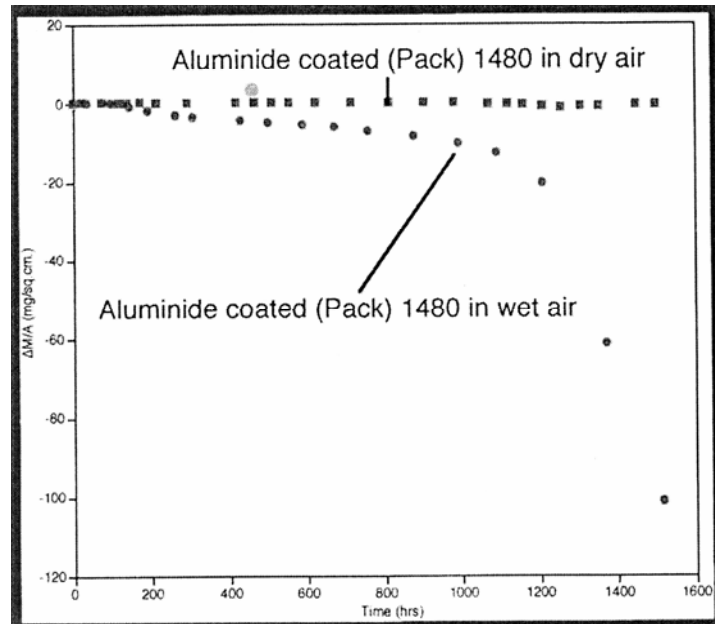


Other Reactants in Gas Affecting Cyclic Oxidation of Alumina Formers

The second reactant causes alumina formation to stop at shorter times

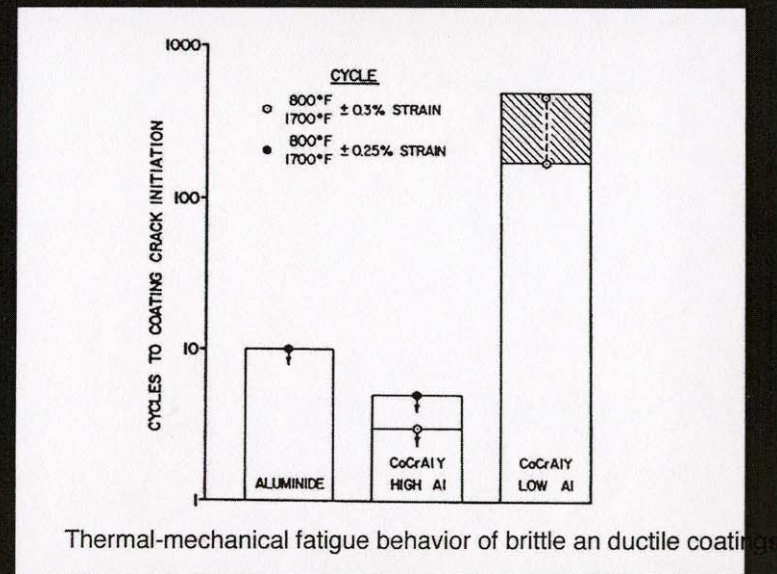
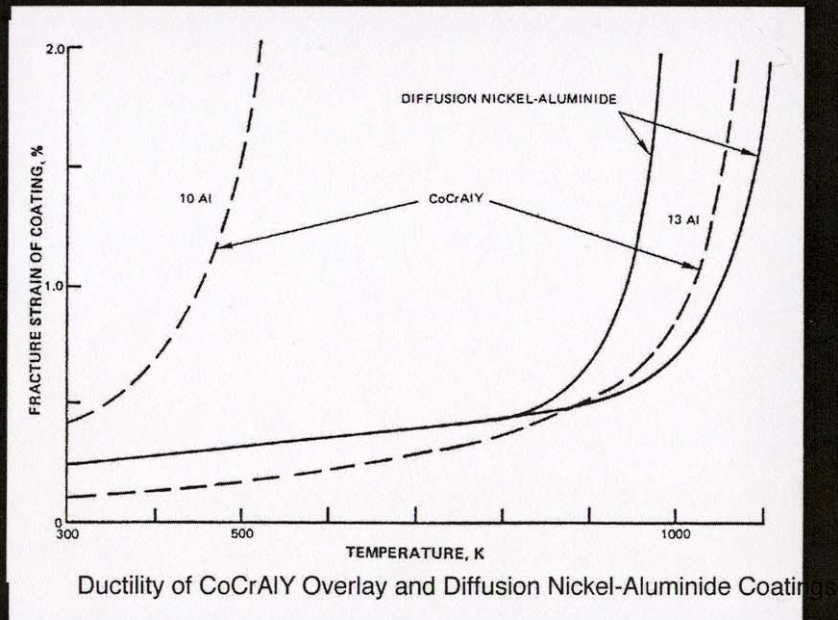


Water Vapor Causes Cracking and Spalling of Alumina to be Increased

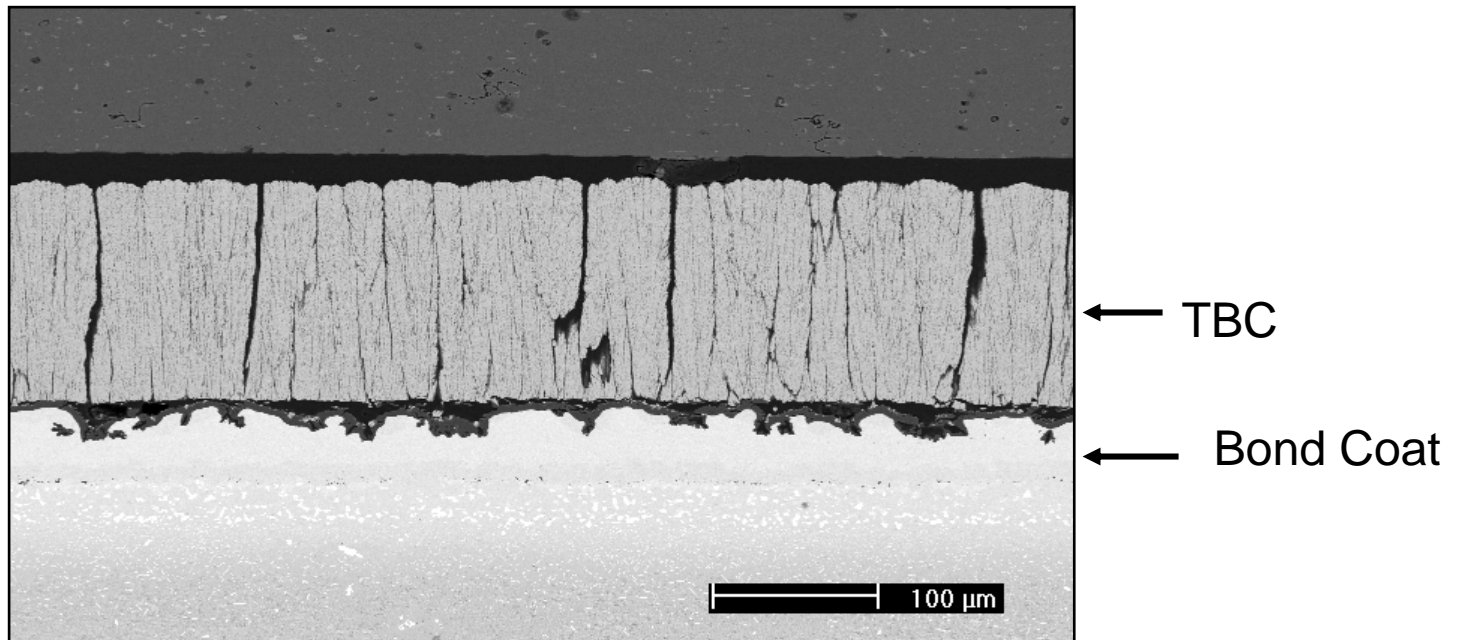


Weight change versus time data for the cyclic oxidation of aluminide coated (by pack Al method) PWA 1480 in wet ($P_{H_2O}=0.1$ atm) and dry air at 1100°C .

Mechanical Properties of Coatings

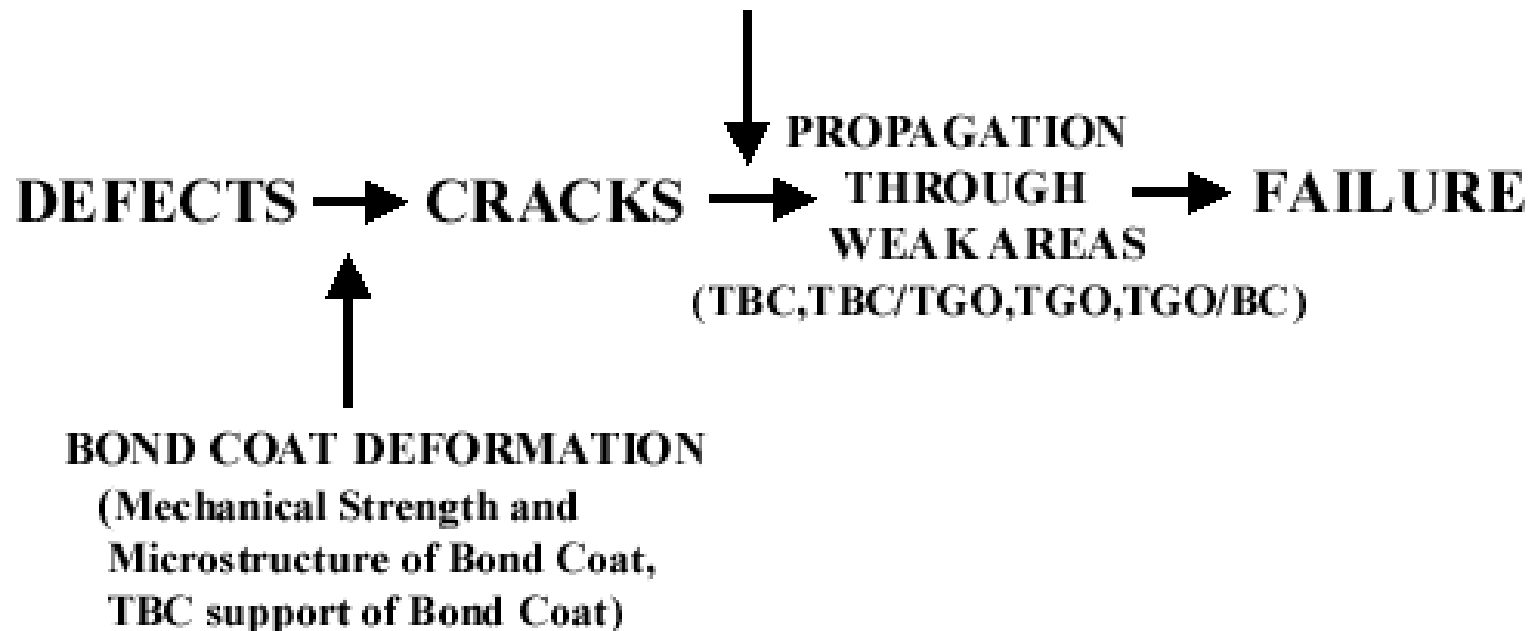


Thermal Barrier Failure at 1100°C

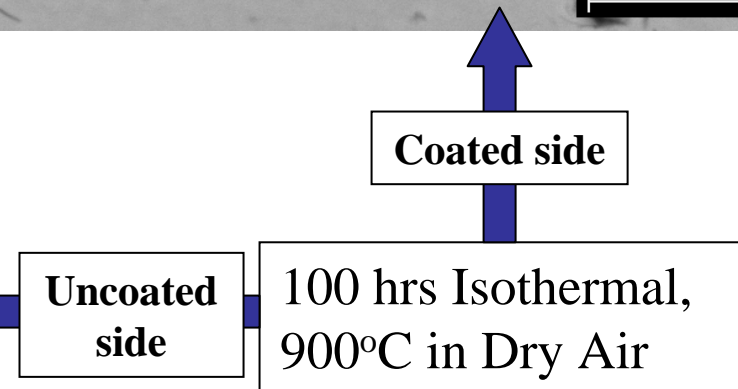
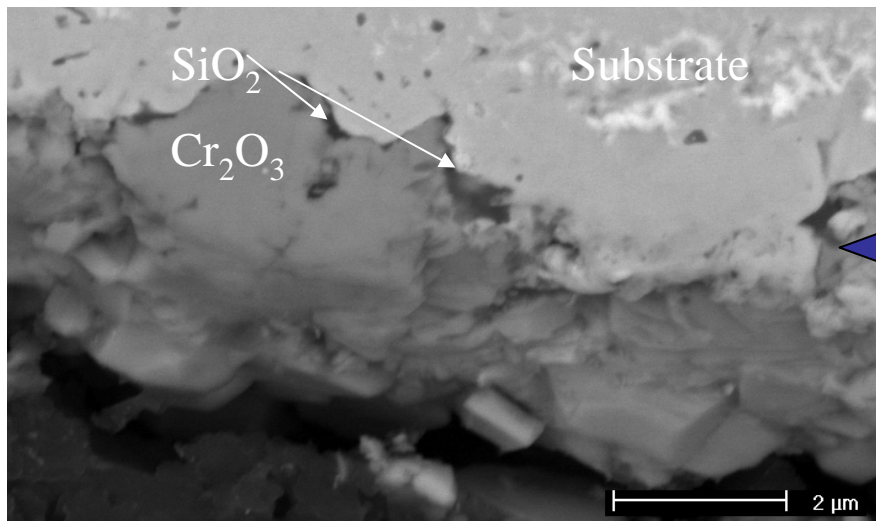
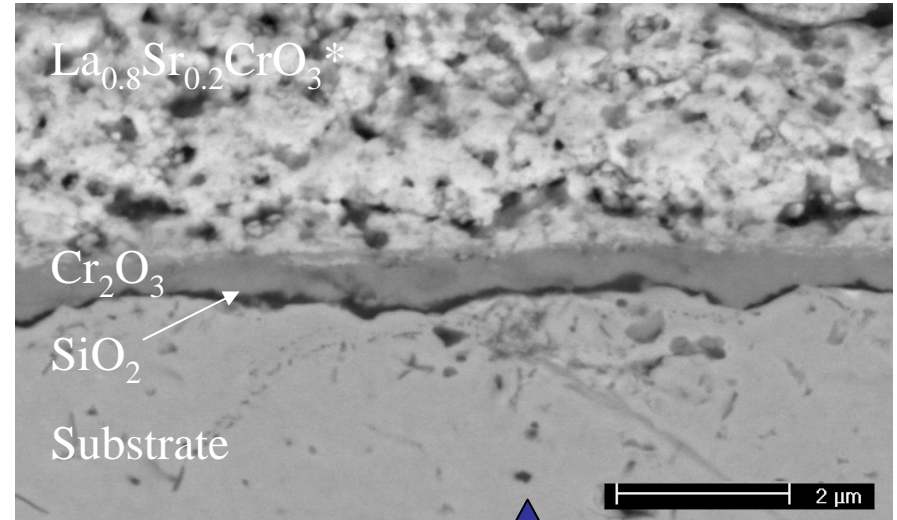
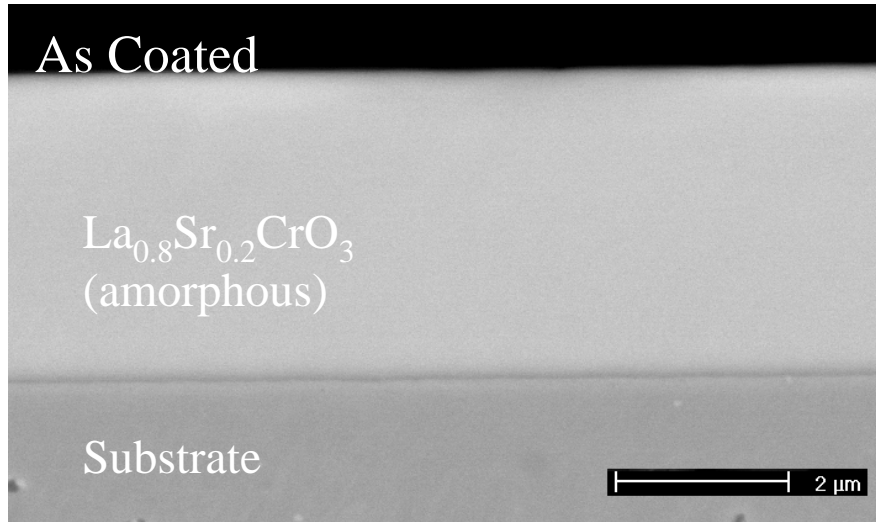


DRIVING FORCE FOR CRACK PROPAGATION

STORED ENERGY IN THE TGO AND TBC

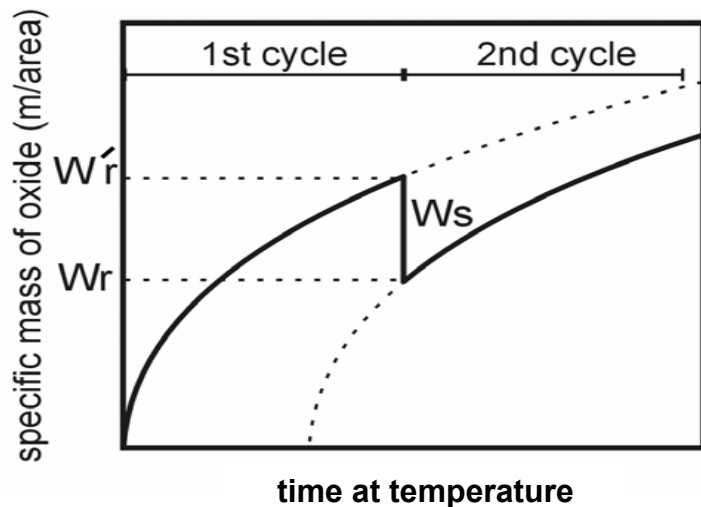
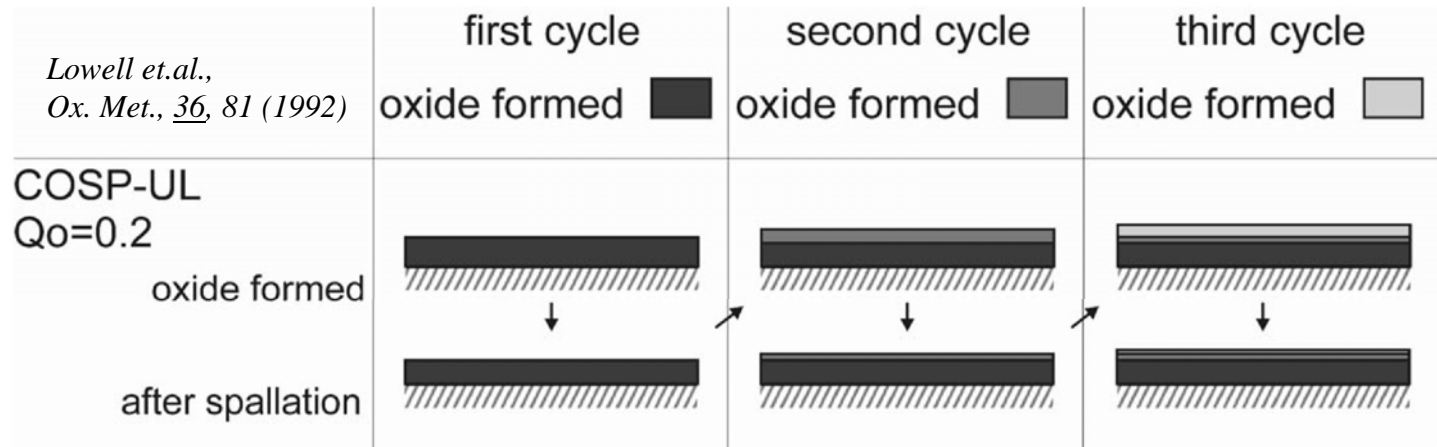


$\text{La}_{0.8}\text{Sr}_{0.2}\text{CrO}_3$ Coated E-Brite (~5mm thick)



*Coating is porous due to a phase transformation during devitrification

Model: COSP-Uniform Layer



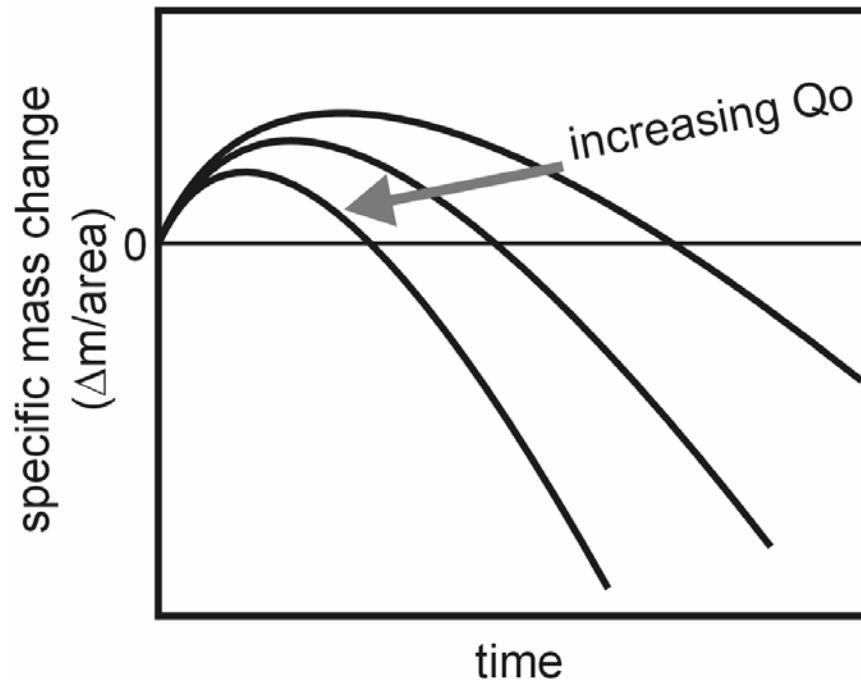
$$F = Q_o \cdot W'r$$

$$W_s = F \cdot W'r$$

$$W_r = W'r - W_s$$

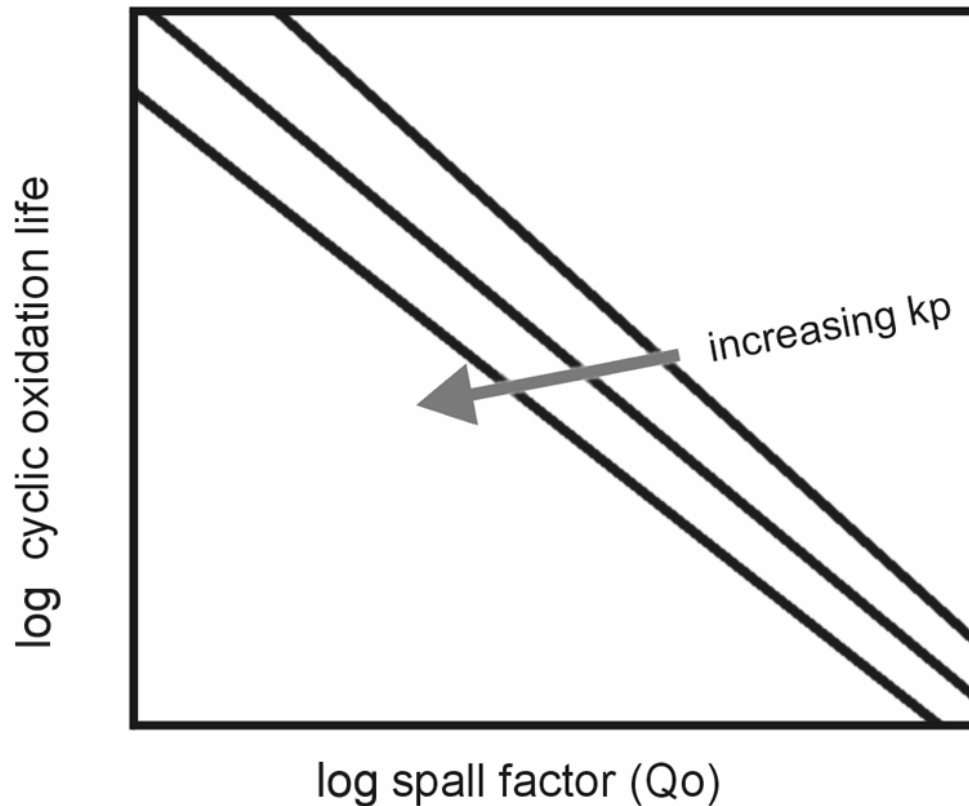
- $W'r$, weight of oxide that forms during the high temperature dwell
- W_s , weight of oxide that spalls during cooling
- W_r , remaining oxide, the starting point of the next cycle
- F , fraction of oxide that spalls
- Q_o , spall parameter

Model: COSP



With known oxide growth kinetics and Q_0 , mass change versus time curves can be constructed

Model: COSP (Life-Time Curves)



Cyclic Oxidation Life

- Cyclic oxidation life is defined as cross over to negative weight change in mass change versus time curves
- Life as a function of oxidation kinetics and spall behavior

COSP and Short-Term Testing

spall factor (Q_o) and experimental variables

$$Q_o = \frac{E^{AE} / A \cdot \rho_{ox}}{B \cdot (W'_r)^2 \cdot \Omega_{ox}}$$

ρ_{ox} oxide density

W'_r weight of retained oxide prior to spallation

E^{AE} acoustic energy

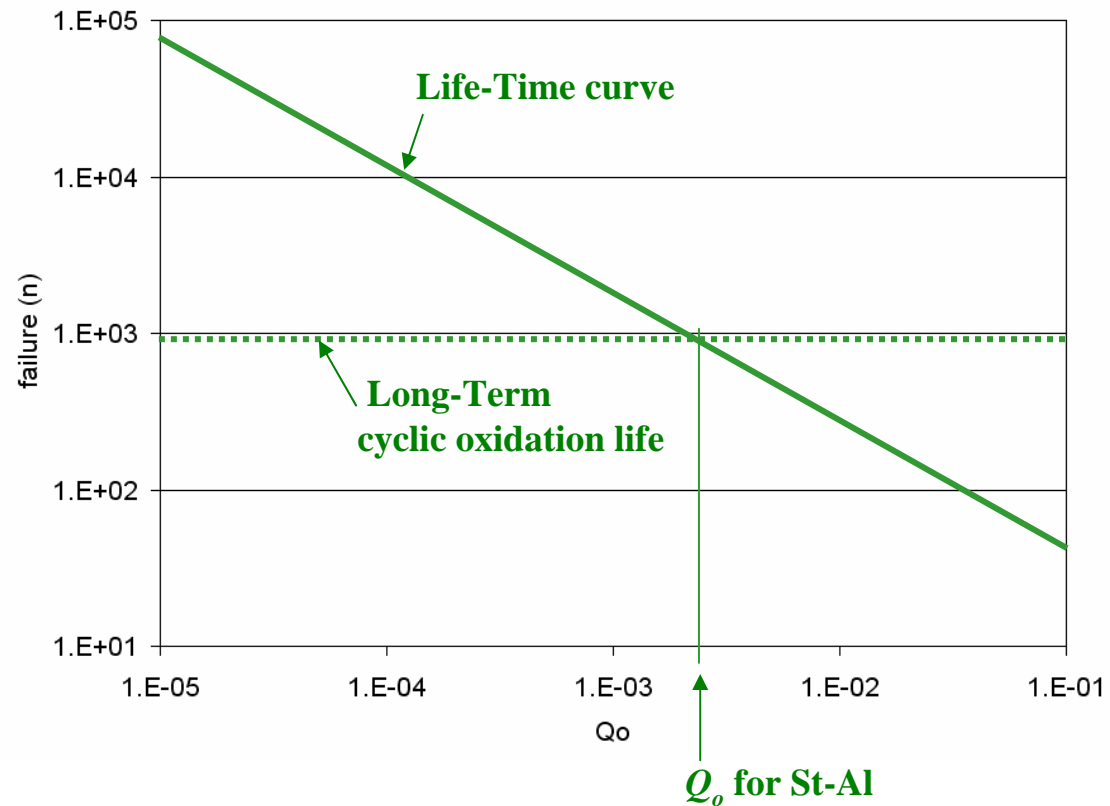
Ω_{ox} elastic strain energy density $\Omega_{ox} = \frac{(1-\nu)}{E} \sigma_o^2$

B ratio of E^{AE} to the fracture energy of oxide spallation

Obtaining B , St-Al

- Long-term cyclic oxidation life
- Life-time curve from COSP
- Q_o from intersection
- Calculate B

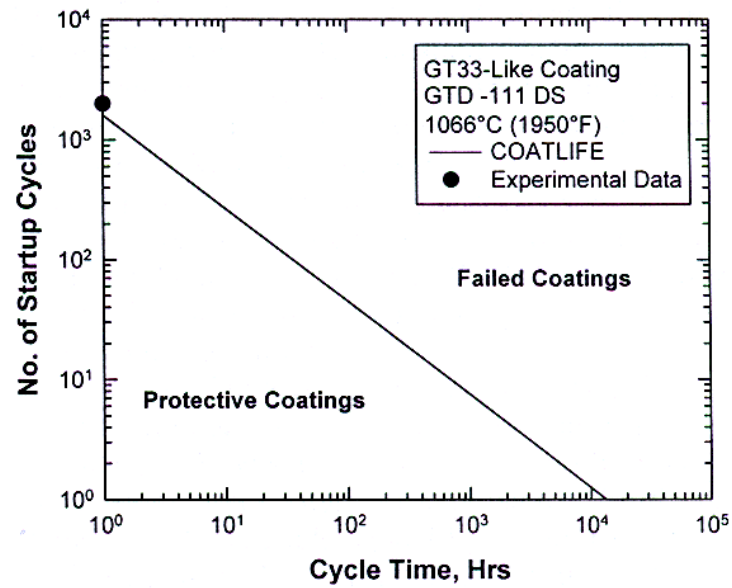
$$Q_o = \frac{E^{AE} / A \cdot \rho_{ox}}{B \cdot (W'_r)^2 \cdot \Omega_{ox}}$$



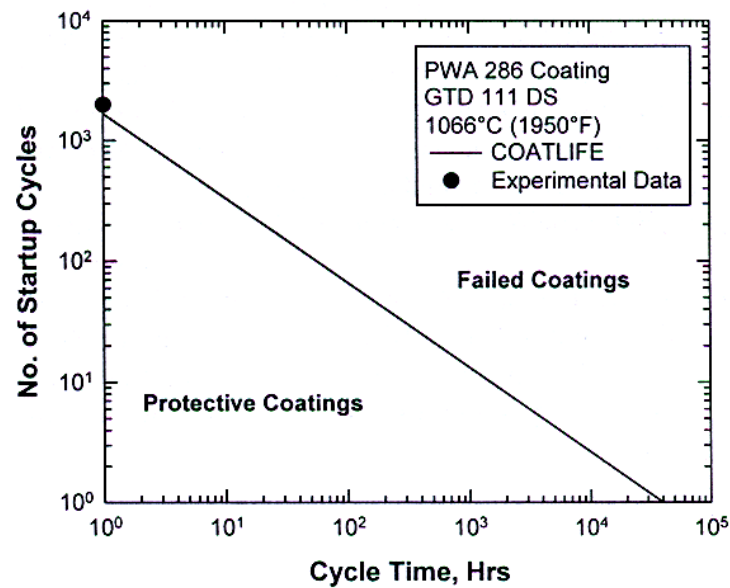
Model Results with Inputs from Short-Term Testing

alloy/coating	cycles to failure (n)	
	experimental long-term test	short-term tests and model
1484	24	64
ls-N5	690	950
st-Al	1000	560
FeCrAlY	>2000 (~4000)	3850
Pt-Al	>4000	10000

MCrAlY Coating Life Diagrams



(a)



(b)

5. Materials for SOFC IC and Selected BOP and Research Direction

IC materials selection

- Requirements
- Alloy selection and design
- Cost

Materials For SOFC, Selected BOP and Research Directions

Requirements

Interconnect Functional Requirements

- Long Term Chemical Stability: 40,000Hrs.
 - High-temperature corrosion / oxidation resistance
 - Oxide Compatibility with Cell Components
- Electrical Performance Stability: ~ 0.1% Voltage reduction
 - Conducting Scale formation
 - Oxide Stability
- Mechanical / Structural Stability
 - Thermal expansion coefficient match
 - Weld / Joint Stability

Material	TEC
YSZ	10-11 x 10 ⁻⁶ /°C
Cr-based alloys	11-12 x 10 ⁻⁶ /°C
400-series stainless steel alloys (Fe-Cr)	12-13 x 10 ⁻⁶ /°C
X10Cr alloys (Fe-Cr-1 Al)	13-14 x 10 ⁻⁶ /°C
Ni-based alloys (Ni>60%)	13-16 x 10 ⁻⁶ /°C
Ni-based alloys (Ni<60%)	16-19 x 10 ⁻⁶ /°C
Other stainless steel alloys (Fe-Cr-5 Al)	15-18 x 10 ⁻⁶ /°C

Alloy Selection and Design

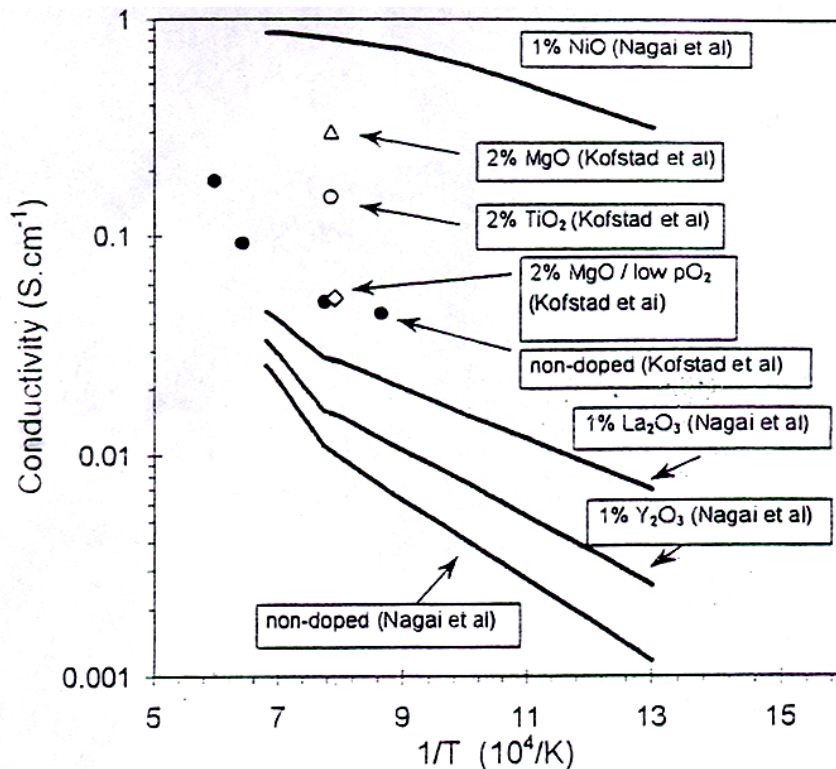
- Major effort is on chromia forming alloys
- Commercial chromia forming alloys are based on the systems NiCr, NiFeCr and FeCr.
- Due to thermal expansion coefficients Fe-Cr alloys have received major emphasis
- Oxide Dispersion Strengthened Chromium has also received some attention.
- A number of ferritic steels have been designed for SOFC Application (Crofer 22APU, JS-3, ZMG 232).

Case Study Crofer

- Chromium concentration sufficiently high to obtain oxidation resistance but not so high as to adversely affect CTE, 22-23%Cr.
- Add reactive element, La, to lower scale growth rate and improve scale adherence.
- Add small amounts of Mn and Ti to obtain external spinel formation to decrease volatile chromium species.
- Ti additions also produce internal oxide precipitates to strengthen alloy adjacent to oxide scale in order to reduce tendency of wrinkling during thermal cycling
- Maintain low Al and Si concentrations to prevent development of Al_2O_3 and SiO_2 discontinuous stringers in the alloy which adversely affect electrical conductivity.

Electrical Conductivity of Chromia Based Scales

- Chromia is an electrical conductor at temperatures greater than 1000°C
- At lower temperatures the concentration of intrinsic electronic defects becomes so small that chromia changes to an extrinsic electronic conductor controlled by the presence of dopants.



Oxide Electrical Properties

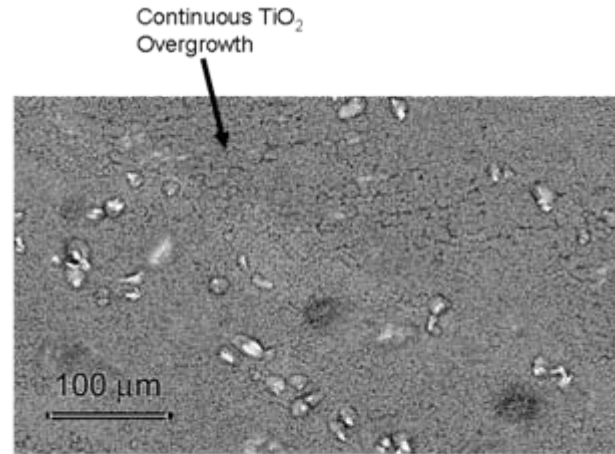
<u>Oxide</u>	<u>ρ (ohm cm) in air</u>
SiO ₂	7 X 10 ⁶ (600°C)
Al ₂ O ₃	5 X 10 ⁸ (700°C)
Cr ₂ O ₃	1 X 10 ² (800°C)
NiO	5 (900°C)
CoO	1 (950°C)
TiO ₂ *	3 X 10 ² (1000°C)

* Note: $\rho_{\text{TiO}_2} = 5 \times 10^{-1}$ ohm cm at $p_{\text{O}_2} = 10^{-16}$ atm

Oxide Vaporization

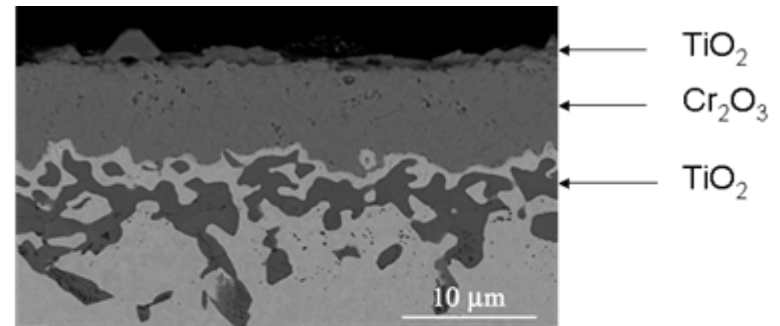
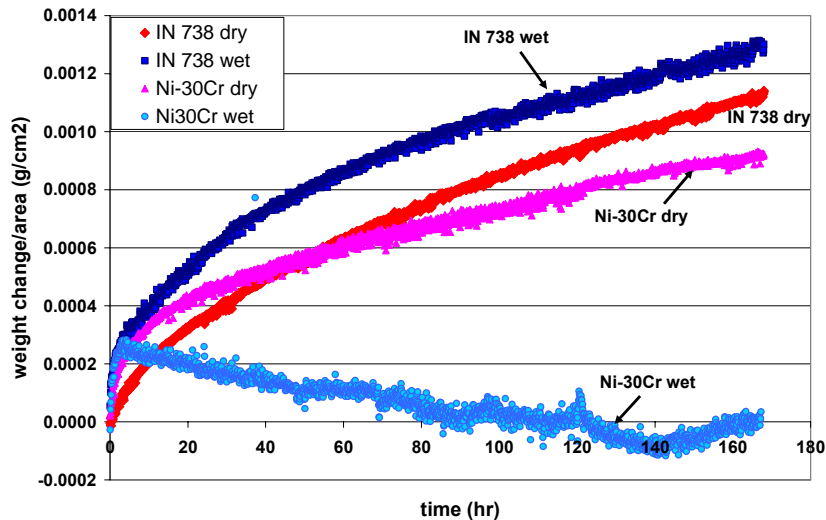
Vapor Pressures – 1100 K

Metal	P_M (atm)	$P_{O_2-M/MO}$ (atm)	Oxide – P_{Oxide} (atm)
Cr	7×10^{-12}	1×10^{-27}	$CrO_3 - 4 \times 10^{-11}$
Fe	1×10^{-12}	9×10^{-20}	$FeO - 1 \times 10^{-16}$
Ni	2×10^{-13}	4×10^{-14}	$NiO - 1 \times 10^{-16}$
Cu	6×10^{-10}	4×10^{-9}	$CuO - 5 \times 10^{-13}$
Ti	1×10^{-15}	4×10^{-36}	$TiO_2 - 1 \times 10^{-20}$



IN 738 at 900°C in wet air (0.1 atm) isothermal-168 hr

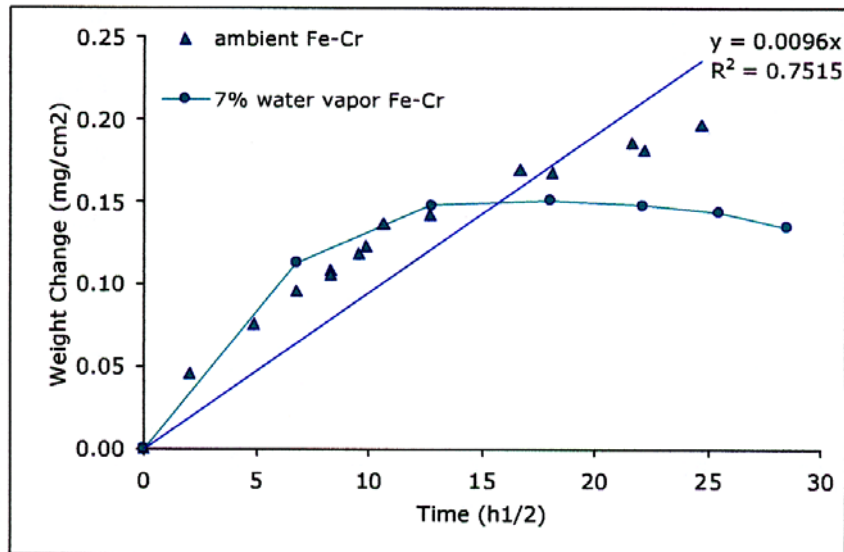
IN 738 and Ni-30Cr at 900C



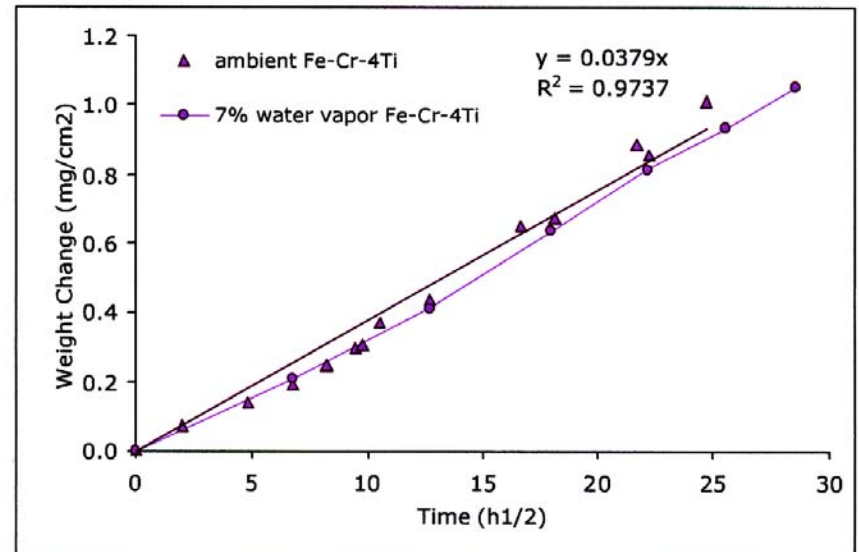
Cross-section of alloy RV2097 after 100 hours at 900°C in dry air.

Cyclic Oxidation

760°C



Fe-22Cr



Fe-22Cr-4Ti

Costs

Prices will move around a lot depending on the cost of various raw materials, particularly Ni and Mo, which drive the cost of the superalloys in particular. Currently Ni is about 7\$/# and Mo is about 30\$/#, which are both high by historical standards. As an aside, most alloying elements are up considerably in price over the last few years and have been showing a lot of volatility.

Product form and general demand/supply also are strong price movers - e.g. plate is generally less expensive than thin sheet, and products which get made in large quantities are generally less expensive than products which are not in demand.

Alloy	Relative price
Basic Fe-Cr stainless steel (e.g. 409ss)	0.5x
High-alloy Fe-Cr stainless steel (e.g. E-BRITE)	2-3x
Basic Fe-Cr-Ni stainless steel (e.g. 304ss)	1
High-alloy Fe-Cr-Ni stainless steel	2-4x
Nickel-base superalloy - corrosion alloys	5-6x
Nickel-base superalloy - heat-resistant alloys	5-9x

J. Rakowski 9/6/05

Testing Requirements

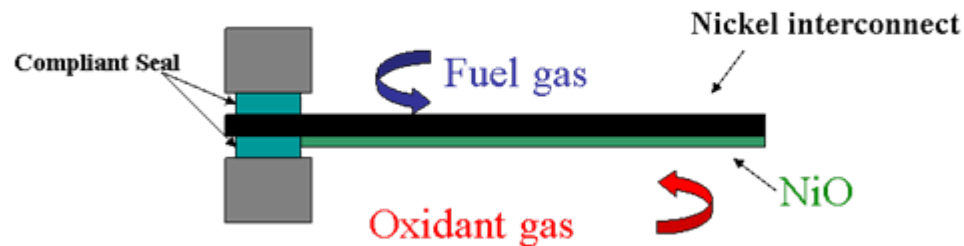
- Dual atmosphere needs to be emphasized
- More testing in typical anode environments is required

Research Directions

- Continue emphasis on chromia formers including electrical conductivity improvements and inhibition of vaporization.

New Directions

Behavior of nickel in a fuel cell environment?



- NiO will form on cathode side, not anode side

Research Directions

Comparison of Ni with Chromia forming alloys

- NiO evaporation is extremely low
- NiO grows faster
- Conductivity dominated by defects
- p_{O_2} dependent
- Chromia contamination from CrO_3 evaporation has produced deleterious effects
- The conductivity of Cr_2O_3 does not have a strong dependence on p_{O_2}

Improving the properties of nickel in a fuel cell environment

- Slow growth rate
 - Coating with reactive element
 - Alloying
- Increase conductivity
 - Doping the scale
- High Conductivity via
 - Ni mesh/silver system
 - Silver studs

Research Directions

Growth of NiO

- Under strong oxidizing environments NiO exists as a metal deficient oxide
- Ni vacancies are the dominant defect
- The growth of NiO is dominated by the outward transport of Ni through the oxide scale.
- The greater the non-stoichiometry, the faster the growth

Reduction of Growth rate

- Grain boundary diffusion plays an increasingly important role in oxide growth as the temperature decreases
- Inhibit grain boundary diffusion by the addition of a reactive element
- The growth of NiO has been reduced by an order of magnitude by coating pre-exposed Ni with Ca, Sr, or other RE
- Pulsed Laser Deposition CeO_2 , SrO

Research Directions

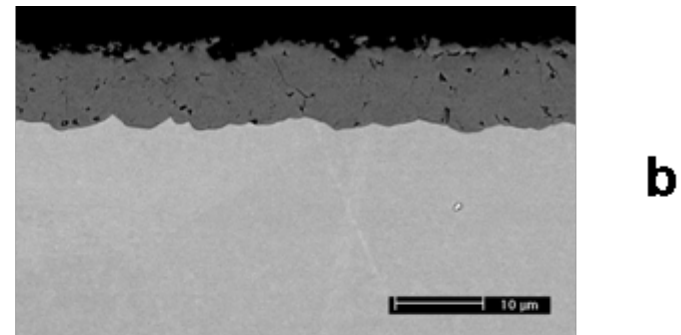
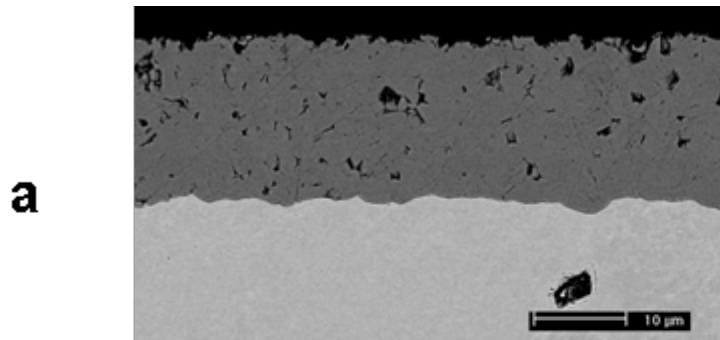
Electrical Conduction of NiO

- $E_g=4.2\text{eV}$, extrinsic behavior
- Ni_{1-x}O , $\text{Ni}^{2+} \rightarrow \text{Ni}^{3+}$ to preserve charge neutrality
- Ni^{3+} provide electron holes, the dominant electrical carrier
- The greater the non-stoichiometry, the greater the conductivity.

Improved Conductivity

- $[\text{Ni}^{3+}]$ is fixed by the oxygen partial pressure
- Doping
 - M^{3+} will increase $[V_m]$, decrease [holes]
 - M^{+} ions will reduced $[V_m]$, increase [holes]
- Ni-5wt%Cu alloy

Research Directions



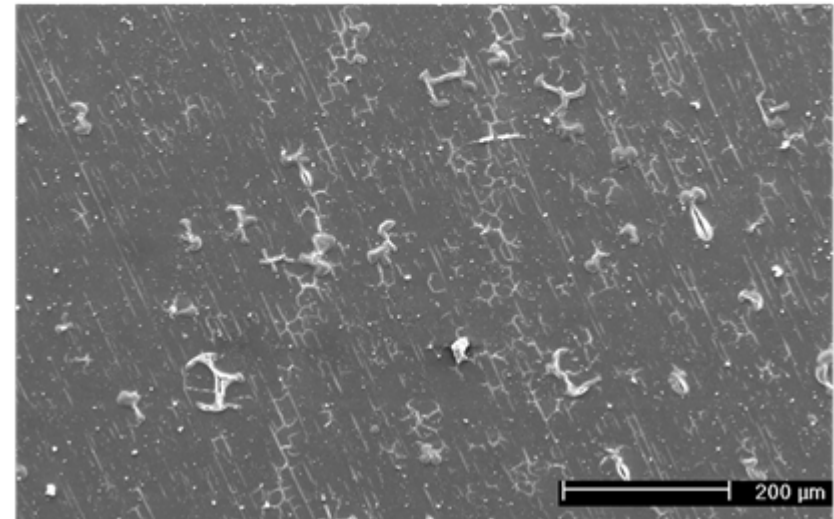
(a) Uncoated nickel, exposed for 100 hours in dry air at 800°C, (b) SrO coated nickel exposed for 100 hours in dry air at 800°C.

Research Directions

SrO coated Ni

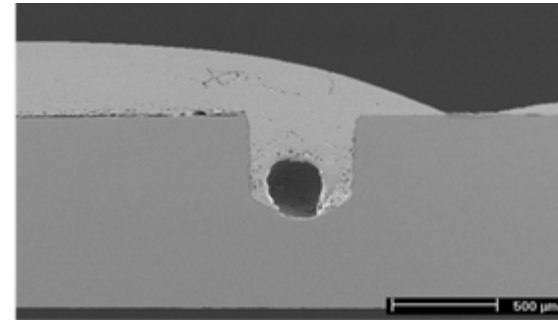
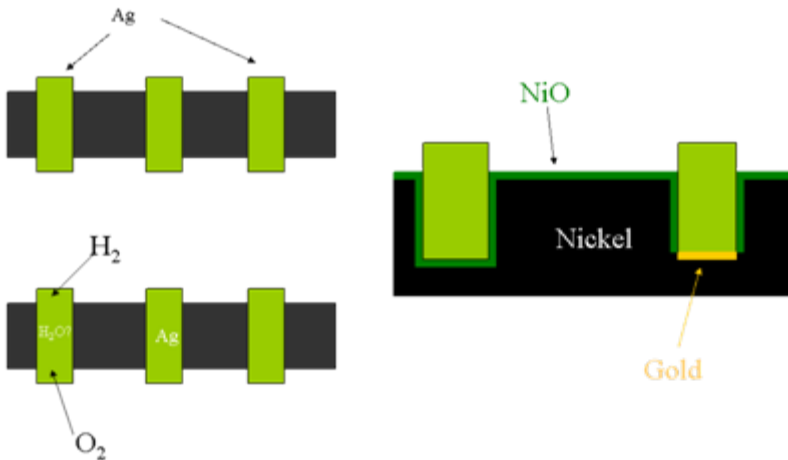
Pulsed Laser Deposition

- 5 minute deposition time
- 10Hz
- ~10 millijoule
- Total pressure 1.6×10^{-2} torr



Research Directions

High Conductivity Via



Silver Via, 800°C 100 Hours, exposed under dual atmospheric conditions. The upper surface was exposed to dry air while the lower surface was exposed to simulated anode gas of Ar-10% H_2O -4% H_2 .